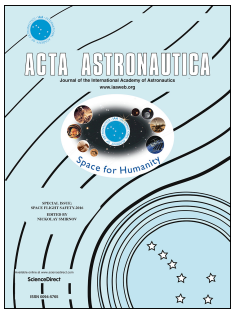

QUEST: A New Frontiers Uranus Orbiter Mission Concept Study

S. Jarmak, E. Leonard, A. Akins, E. Dahl, D.R. Cremons, S. Cofield, A. Curtis, C. Dong, E.T. Dunham, B. Journaux, D. Murakami, W. Ng, M. Piquette, A. Pradeepkumar Girija, K. Rink, L. Schurmeier, N. Stein, N. Tallarida, M. Telus, L. Lowes, C. Budney, K.L. Mitchell

PII: S0094-5765(20)30041-2

DOI: https://doi.org/10.1016/j.actaastro.2020.01.030

Reference: AA 7854

To appear in: *Acta Astronautica*

Received Date: 31 May 2019

Revised Date: 10 December 2019

Accepted Date: 20 January 2020

Please cite this article as: S. Jarmak, E. Leonard, A. Akins, E. Dahl, D.R. Cremons, S. Cofield, A. Curtis, C. Dong, E.T. Dunham, B. Journaux, D. Murakami, W. Ng, M. Piquette, A.P. Girija, K. Rink, L. Schurmeier, N. Stein, N. Tallarida, M. Telus, L. Lowes, C. Budney, K.L. Mitchell, QUEST: A New Frontiers Uranus Orbiter Mission Concept Study, *Acta Astronautica*, https://doi.org/10.1016/j.actaastro.2020.01.030.

QUEST: A New Frontiers Uranus Orbiter Mission Concept Study

S. Jarmak[a*], E. Leonard[b,c], A. Akins[d], E. Dahl[e], D. R. Cremons[f], S. Cofield[g], A. Curtis[c], C. Dong[h], E. T. Dunham[i], B. Journaux[j], D. Murakami[k], W. Ng[l], M. Piquette[m], A. Pradeepkumar Girija[n], K. Rink[c], L. Schurmeier[o], N. Stein[p], N. Tallarida[c], M. Telus[q], L. Lowes[c], C. Budney[c], K. L. Mitchell[c]

[a]*University of Central Florida, United States*
[b]*University of California Los Angeles, United States*
[c]*Jet Propulsion Laboratory, California Institute of Technology, United States*
[d]*Georgia Institute of Technology, United States*
[e]*New Mexico State University, United States*
[f]*NASA Goddard Space Flight Center, United States*
[g]*Old Dominion University, United States*
[h]*Princeton University, United States*
[i]*Arizona State University, United States*
[j]*University of Washington, United States*
[k]*NASA Ames Research Center, United States*
[l]*University of Maryland, United States*
[m]*University of Colorado Boulder, United States*
[n]*Purdue University, United States*
[o]*University of Illinois Chicago, United States*
[p]*California Institute of Technology, United States*
[q]*University of California Santa Cruz, United States*

ABSTRACT

The ice giant planets, Uranus and Neptune, are fundamentally different from the gas giant and terrestrial planets. Though ice giants represent the most common size of exoplanet and possess characteristics that challenge our understanding of the way our solar system formed and evolved, they remain the only class of planetary object without a dedicated spacecraft mission. The inclusion of a Uranus orbiter as the third highest priority Flagship mission in the NASA Planetary Science Decadal Survey "Vision and Voyages for Planetary Science in the Decade 2013–2022" indicates a high level of support for exploration of the ice giants by the planetary science community. However, given the substantial costs associated with a flagship mission, it is critical to explore lower cost options if we intend to visit Uranus within an ideal launch window of 2029 - 2034 when a Jupiter gravity assist becomes available. In this paper, we describe the Quest to Uranus to Explore Solar System Theories (QUEST), a New Frontiers class Uranus orbiter mission concept study performed at the 30th Annual NASA/JPL Planetary Science Summer Seminar. The proposed QUEST platform is a spin-stabilized spacecraft designed to undergo highly

elliptical, polar orbits around Uranus during a notional one-year primary science mission. The proposed major science goals of the mission are (1) to use Uranus as a natural laboratory to better understand the dynamos that drive magnetospheres in the solar system and beyond and (2) to identify the energy transport mechanisms in Uranus' magnetic, atmospheric, and interior environments in contrast with the other giant planets. With substantial mass, power, and cost margins, this mission concept demonstrates a compelling, feasible option for a New Frontiers Uranus orbiter mission.

Keywords: Uranus, Planetary Science Summer Seminar, Ice Giants, Orbiter Mission Concept Study, New Frontiers

*Corresponding author. E-mail address: Jarmak@knights.ucf.edu (S. Jarmak).
Permanent address: 4283 Shadow Creek Circle Oviedo, FL 32765

1. Introduction

The ice giants, Uranus and Neptune, represent the only major class of planetary objects in our solar system that have yet to be targeted by a dedicated spacecraft. The only direct measurements of these planets' environments were made during the Voyager 2 flybys in 1986 and 1989 for Uranus and Neptune, respectively. This brief glimpse of Uranus and Neptune over 30 years ago revealed enigmatic worlds that demand missions singly devoted to unraveling their mysteries. Uranus in particular, with its tilted magnetic field, inexplicably hot stratosphere, anomalously low heat flux, and puzzling interior, serves as an extreme environment in which we can test hypotheses for the way our solar system formed and evolved [1, 2, 3]. Ice giant-sized planets also represent a large and growing category of recently discovered exoplanets [4]. Remote sensing and in situ measurements of the ice giants in our own solar system would significantly aid our understanding of exoplanetary ice giants, including the composition of their interiors, the thermal structure of their atmospheres, and the surface processes of their satellites that may harbor subsurface oceans. Though most detected ice giant-size planets orbit close to their host star due to observational bias, comparisons between ice giant planets at different distances from their host star could yield a deeper understanding of ice giant evolution and potential migration within solar systems. Our understanding of these exoplanets and their roles in their respective planetary systems would improve through further investigation of the ice giants in our own solar system. Therefore, if we hope to understand the conditions necessary to produce the observed diversity of planets in our solar system and beyond, it is imperative that we return to this frozen frontier.

The NASA JPL Planetary Science Summer Seminar (PSSS) provides early career scientists and engineers with hands-on experience in the end-to-end mission design process. The participants respond to the most recent

NASA Science Mission Directorate New Frontiers Announcement of Opportunity (New Frontiers 4 [5] for our study) and select a high-priority mission target based on community recommendations provided by the NASA Planetary Science Decadal Survey [6]. The seminar consists of 11 weeks of preparatory webinars and group sessions during which the participants design a preliminary mission concept for their chosen target through continual development of a broad set of potential mission goals, mission architectures, and instruments. The PSSS culminates in a 5-day session at JPL where participants work with JPL's advanced project design team, "Team X", to refine the mission concept through spacecraft design, instrument design, trajectory optimization, and trade analyses to ensure the mission fits within predetermined mass, power, and cost caps while achieving a preponderance of community-driven high-priority science objectives.

As participants of the 2018 PSSS, we selected Uranus as our mission target and designed a Uranus orbiter mission concept within a New Frontiers budget adjusted for inflation ($900 M FY18). A Uranus orbiter is ranked as the third priority flagship class mission in the most recent Decadal Survey after a Europa orbiter and Mars sample return mission. Two flagship missions are currently under development, Europa Clipper and Mars 2020, but the budget for NASA planetary exploration missions is not guaranteed to support a third flagship class mission within the ideal launch window of 2029 - 2034 for a mission to Uranus. Therefore, if we want to investigate Uranus within this timeframe it is crucial to determine whether a mission with a significantly reduced budget can achieve sufficiently compelling science to justify the associated cost.

Several recent ice giant mission concept studies have been carried out including the 2019 ESA study "A Mission to the Ice Giants - Uranus and Neptune" [7], the joint NASA/ESA 2017 Ice Giants Pre-Decadal Mission Study Report [8], and two Uranus orbiter concept studies, MUSE [9] and OCEANUS [10], carried out during the 2014 and 2016 PSSS respectively. However, each of these mission concepts arrived at costs greater than 1.2 billion dollars, and several of these studies described as New Frontiers mission concepts include significantly increased cost caps along with donated instruments that obfuscate the true mission costs. In our study, we sought to provide the planetary exploration community with a mission concept that adhered to the New Frontiers guidelines as strictly as possible to present a realistic view of the science achievable at Uranus for less than 900 M FY18$. We were able to meet that goal through the choice of an optimal trajectory that utilizes a Jupiter gravity assist for a launch in 2032, a mission architecture based significantly on the Juno mission, and a focused, synergistic set of goals. Additionally, we found it was necessary to focus on the ice giant itself and limit the rings and satellites science to opportunistic

measurements to fit within New Frontiers constraints while achieving goals related to Uranus' atmosphere, interior, and magnetosphere.

The New Frontiers program does not currently include the ice giants as possible exploration targets; we support the recommendation made by several planetary assessment groups [11, 12] and the Ice Giants Pre-Decadal Mission Study Report [8] that NASA should open New Frontiers to all mission concepts that address high-priority science questions from the NASA Decadal Survey. In our study, we found that, given the dearth of knowledge associated with the Uranian system, even a spacecraft limited to a New Frontiers budget equipped with a modest instrument suite would yield valuable insights regarding the origin and evolution of our solar system as well as a greater understanding of physical processes critical to the sustainability of habitable environments.

In this paper, we describe our New Frontiers Uranus orbiter mission concept, QUEST (mission logo shown in Figure 1). Section 2 provides the scientific background and motivation for our mission along with the mission science goals and objectives. Section 3 describes our selected instrument suite and spacecraft design. Section 4 describes the chosen launch trajectory and observation schedule of the mission. Section 5 outlines the mission cost, risk, and mitigation strategies.

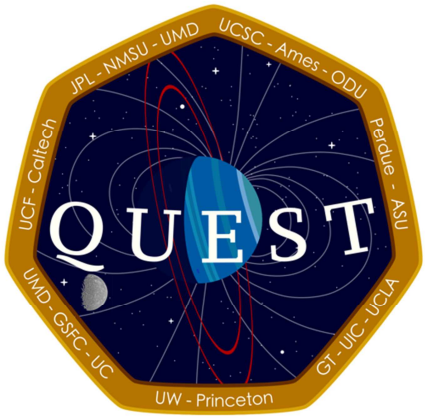

Figure 1. The QUEST mission logo designed by participant Baptiste Journaux depicting the Uranus environment including its obliquity and unique offset magnetic field. The heptagon design represents Uranus as the 7th planet and was inspired by the New Horizons nonagon mission patch.

2. Science Background, Goals, and Objectives

In this section, we provide scientific background and motivation for a focused mission to Uranus along with the current state of knowledge of Uranus' atmosphere, magnetosphere and interior, and the open questions that motivate the QUEST mission concept goals and objectives.

2.1 Science Background and Motivation

Results from the Voyager 2 flyby during solstice at Uranus' southern pole have provided significant insight into the nature of the Uranian system [13]. Multi-wavelength imaging and occultation observations revealed the thermal structure, bulk composition, and dynamics of the atmosphere as well as the material and size properties of the ring particles, satellite surface features, and new Uranian satellites. Additionally, the Voyager 2 plasma, charged particle, and magnetometry experiments gave a preliminary look into the structure and physics of the magnetosphere, as well as the interactions of charged particles with the rings and satellites. In addition to the axial tilt of Uranus itself, the magnetic dipole is both highly inclined (59 degrees with respect to the rotation axis) and off-center (generated 70% away from Uranus' center). These properties, along with the relatively large observed quadrupole contribution to the magnetic field, suggest a unique dynamo structure potentially generated in "oceanic" regions of the planet [14]. Furthermore, the heat flux originating from the interior of Uranus is low when compared to the other planets in the solar system, with a net energy balance (ratio of emitted thermal flux and the absorbed solar flux) of 1.06 ± 0.08 [15]. This implicates seasonal forcing as the primary driver of meteorological activity [1]. Despite several attempts, a currently proposed model of the interior which agrees with all of the Voyager observations does not exist [1]; thus, we do not have a clear picture of how Uranus formed and evolved to its current state. A focused set of measurements investigating Uranus' atmosphere, magnetosphere and interior is therefore necessary to place Uranus in the context of our solar system's formation and subsequent evolution.

Though Uranus and Neptune are both ice giant planets, they possess many distinguishing physical characteristics. Uranus's extreme obliquity leads to unusual seasonal processes not observed on Neptune, and its complex magnetic field suggests an exotic interior dynamo. While Neptune possesses interesting qualities worthy of a dedicated mission, including its largest moon Triton which is currently hypothesized to be a captured Kuiper Belt Object, Uranus is arguably a more attractive target. Uranus is closer (19 vs 30 AU) allowing for a shorter cruise duration and less massive camera designs due to light availability; it is the only giant planet whose interior has not adequately been described by a simple 3-layer model [16, 17]; its high obliquity (98 degrees compared to 28 degrees at Neptune) produces a more extreme atmospheric and magnetic environment; and it is the only planet for which

observations are consistent with zero internal heat output [15]. Focused measurements of Uranus' environment would therefore provide ground truth for the thousands of extreme exoplanetary environments observed and yield a deeper understanding of the fundamental processes that produce the observed diversity of planets in our galaxy.

The question as to whether Uranus formed close to its current location or closer to the Sun before migrating outwards is still an outstanding issue [18, 19, 20]. Further estimates of the bulk abundances of the common elements (Carbon, Oxygen, Nitrogen, Sulfur) can provide constraints on Uranus' formation location. Current knowledge of heavy element (*i.e.*, heavier than He^4) abundances in the atmosphere of Uranus is severely limited in comparison to the gas giants, especially Jupiter, due to a lack of dedicated spacecraft observations of the ice giants. Ground-based observations have constrained Uranus' C/H ratio based on atmospheric methane abundance to 50 to 100 times the solar value [21], and no firm constraints exist for Nitrogen, Oxygen, or Sulfur [22]. In addition to Carbon, Oxygen, Nitrogen, and Sulfur, noble gas (Helium, Argon, Krypton, Neon, and Xenon) abundances and their comparison to solar, protosolar, and gas giant abundances would provide evidence to distinguish between formation hypotheses (*i.e.* disk instability vs. core accretion) [3]. While they are uniformly mixed in the upper atmosphere, noble gasses are not measurable via remote sensing and would require an *in situ* atmospheric probe with a sensitive mass spectrometer, which we deemed outside the scope of our study. Similarly, models of the interior structure and dynamo inferred from the observed characteristics of the magnetic field can constrain the properties of Uranus' early formation environment and yield further weight to hypotheses seeking to explain its axial tilt. Additionally, observations of Uranus' thermal structure at equinox and its latitudinal and longitudinal variations can determine the localization extent of convective activity, complementing the Voyager 2 observation at solstice and providing a deeper look into Uranus' unique atmospheric dynamics. The conditions of Uranus' formation and migrational history, and therefore the formation and evolution of our solar system, can be greatly elucidated through dedicated observations of temporal and spatial variations in Uranus' atmosphere, magnetic field, and interior.

2.1.1 Atmosphere

Recent ground-based and space-based observations of Uranus' atmosphere have revealed a dynamic environment in stark contrast to the serene world observed by Voyager 2. Recent discoveries include the presence of persistent storm clouds [23, 24] and significant methane depletion at the poles, suggestive of seasonally-varying meridional circulation [25] (recent observations of this dynamic atmosphere are shown in Figure 2).

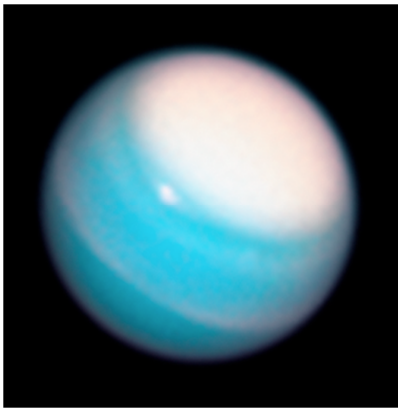

Figure 2. Hubble Space Telescope image taken in September 2018 revealing Uranus' vast polar cap and a bright, persistent storm. Credits: NASA, ESA, A. Simon (NASA Goddard Space Flight Center), and M.H. Wong and A. Hsu (University of California, Berkeley).

In addition, surface winds observed by long-exposure near-infrared imaging of Uranus near equinox show a banded structure similar to that of Jupiter (Figure 3), where the Juno mission has shown winds that extend deep into the planet's atmosphere [26]. With imaging and microwave radiometry capabilities, QUEST is well-positioned to elucidate the relationship between these surficial features and the circulation and thermal environment of the deep atmosphere, which is still largely unconstrained in composition and dynamism [1]. Mapping of any convective cells in the troposphere and in the interior of the planet's atmosphere by measuring the spatial distribution of gas abundances at depth could also aid in determining the source of the planet's oddly-shaped and temporally-changing magnetic field, which may be linked to turbulence in the planet's deeper layers [27].

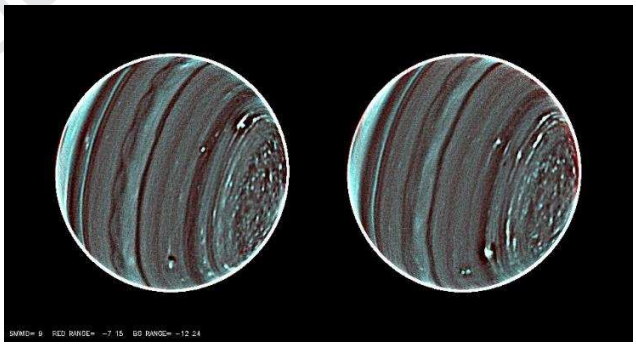

Figure 3. High contrast near-infrared Keck telescope observations of Uranus in 2012 revealing distinct clouds and banded structures similar to the other giant planets in contrast with the seemingly passive exterior observed during the Voyager 2 flyby in 1986. Credit: NASA / ESA / L. A. Sromovsky / P. M. Fry / H. B. Hammel / I. de Pater / K. A. Rages.

Adding to the complexity of the atmosphere is the anomalously low thermal emission observed by Voyager 2, which is almost equal to the incident solar flux, and the cause of which is still unknown [15]. Competing hypotheses for the low thermal emission include the presence of thermal boundary layers in the atmosphere [28], a

conductive layer in the deep atmosphere [29], or internal stratification [17], possibly due to a giant impact that gave Uranus its unusual axial tilt [30]. To constrain these models, QUEST would use microwave receivers designed to probe the deep atmosphere of Uranus for conductive or boundary layers. From these measurements, the gas volume mixing ratios of ammonia and hydrogen sulfide as a function of atmospheric depth and latitude could be extracted, giving insight into deep atmospheric circulation and the atmospheric lapse rate that may help explain the observed low thermal emission. Understanding the coupling of the observed surficial atmospheric features to the deep atmosphere and hypothesized supercritical layers is paramount to developing a self-consistent dynamical model of Uranus, and this model can also be used to inform models of the abundance of ice giant exoplanets already discovered.

Voyager 2 radio and stellar occultations also revealed that the stratosphere of Uranus was unexpectedly warm. The introduction of various absorbers into the atmosphere, including methane and haze layers, into radiative convective models was unable to attribute this warmth to a single source, and it is possible that heat transfer from the thermosphere would be necessary to achieve the observed atmospheric structure [31]. QUEST would observe the high latitude thermal structure of Uranus during equinox via radio occultation, taking advantage of the X and Ka band telecommunications subsystem to obtain further constraints on the thermal structure of the thermosphere and lower stratosphere.

2.1.2 Magnetosphere

The Voyager missions revealed that the ice giants appear to have distinct magnetic fields from gas giants and terrestrial planets (Figure 4). Voyager 2 measurements indicated that Uranus' magnetic field can be characterized to first order as a tilted (59 degrees with respect to the rotation axis), offset (by 1/3 Uranus radii) dipole. In a spherical harmonics representation, the ice giants are dominated by quadrupole and octupole components in contrast to the terrestrial and gas giant planets that are dominated by dipole contributions [32]. The Juno and Cassini missions have provided detailed mapping of the magnetic fields of Jupiter and Saturn, respectively, and have shown that, despite the similarity of Jupiter and Saturn as gas giants, these planets produce markedly different magnetic fields [33, 34] These differences are currently being explored through investigations associated with the planets' interiors, but to gain a full understanding of dynamo generation in our solar system would require similarly detailed mapping of the ice giants. The Juno mission was able to resolve the internal field at Jupiter to

order 10 after 9 orbits [35]. Our proposed mission would follow the same approach as Juno and would resolve up to spherical harmonic order 10 for Uranus' magnetic field.

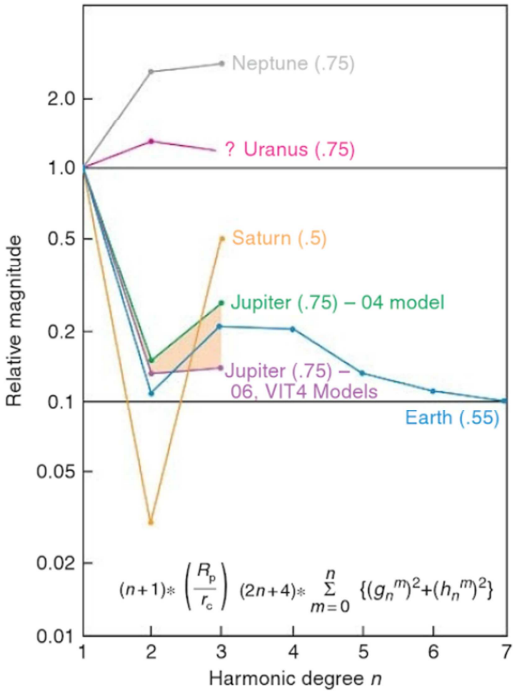

Figure 4. Relative harmonic content of spherical harmonic models of Jupiter, Saturn, Uranus and Neptune compared to Earth, normalized to the assumed core radius for each planet [32].

The angle between Uranus' magnetic dipole axis and planetary rotation axis is the largest of any of the planets in our solar system. This offset results in a unique magnetospheric configuration that has a significant effect on the resulting dynamics. Uranus' magnetosphere is dominated by solar wind-driven magnetospheric convection, but the planet's rapid rotation (17.2 hours) for its size (4 times the size of Earth) indicates that rotation-driven dynamics may be important as well [36, 37]. The complex geometry of the system (Figure 5) results in a magnetosphere that tumbles asymmetrically with respect to the solar wind, and it is currently hypothesized that Uranus' magnetosphere connects with this magnetized solar wind on the order of its ~17-hour rotation period resulting in a magnetosphere that opens and closes on a daily basis [38]. Understanding how Uranus' magnetosphere is coupled to the solar wind is critical to identifying energy transport mechanisms within the system. Unraveling these processes, particularly in contrast to the magnetic interactions ongoing at the other giant planets, will provide further evidence to support current models of magnetospheric dynamics. Additionally, the study of the solar wind-

Uranus interaction may also facilitate our understanding of the stellar wind-planet interaction of exoplanets with high magnetic obliquities [39, 40] thereby expanding our magnetospheric comparative planetology capabilities beyond our own solar system.

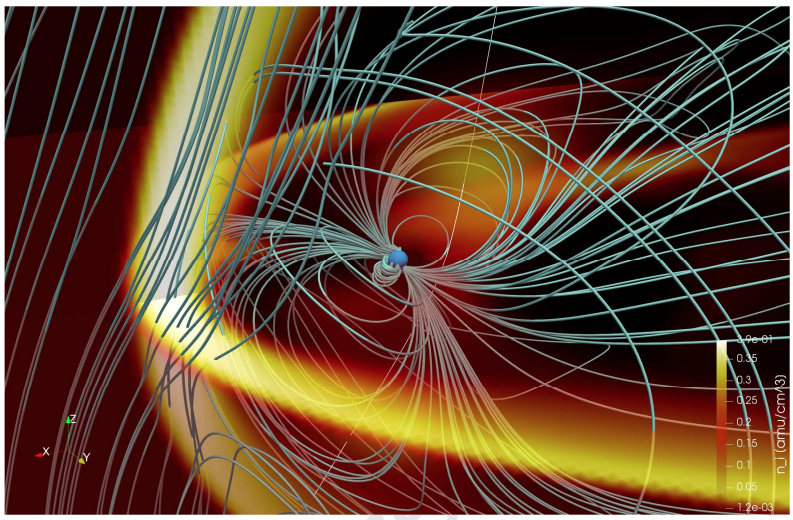

Figure 5. Depiction of Uranus' complex magnetic field interaction with incident solar wind from the ten-moment multifluid magnetosphere simulation (for model details, please refer to [41, 42, 43]. The color contours depict the proton density in cm^{-3}. The magnetic field lines are presented in cyan. Open and closed field lines on the dayside magnetosphere result from magnetic reconnection between the interplanetary magnetic field and planetary magnetic field.

Additionally, Voyager 2 arrived when Uranus was near northern summer solstice [44] and the proposed arrival date of 2045 for the QUEST mission would be near the autumnal equinox. Uranus' magnetosphere therefore provides an excellent laboratory for studying diurnal and seasonal variability of magnetospheric dynamics in our solar system and beyond.

2.1.3 Interior

While both the ice and gas giants have compositionally similar atmospheres (primarily hydrogen and helium), current models of their interiors differ significantly. Current models of ice giant interiors employ a three-layered structure with a small rocky core, an inner envelope composed predominantly of water, methane, and ammonia high-pressure ices, and an outer gaseous envelope comprising the atmosphere [20, 29, 45]. These models are constrained by measurements of the total mass, the equatorial radius and the gravitational moments, but are also additionally informed by other observables such as the one bar temperature, the luminosity, the angular velocity, the magnetic field and the atmospheric abundances of volatile species. However, structural models of Uranus in particular have failed to agree overall with available gravity, magnetic field, and thermal emission measurements [1]. It is worth noting, however, that the one bar temperature was determined through Voyager 2 occultation

measurements, providing only a single data point in time and space, and additional measurements provided by a dedicated mission would yield improved constraints for models of Uranus' interior.

Uranus' magnetic field, like that of other magnetically-active planets, is thought to be generated by convective motions of conductive material within the interior. A number of experimental and numerical studies have shown that water becomes electrically conductive under high pressure due to the mobility of protons, e.g. [46, 47, 48]. Thus, the presence of a magnetic field at Uranus suggests that a layer of high-pressure water - instead of conductive metals - serves as the conductive material. In addition, theoretical and numerical calculations predict that the magnetosphere at solstice would transform periodically between an open and a closed structure [38, 49]. However, additional in situ measurements are required to validate this hypothesis. Since Uranus' magnetic field is multipolar, however, the dynamo action region is likely relatively shallow, unlike those of the Earth and the gas giants. It has also been suggested that the fluid motions of the interior conducting region could be dynamically coupled to the deep atmosphere of Uranus, generating atmospheric wind features that would be seen at the surface [27]. However, observational constraints [50] suggest that the dynamics are limited to the upper 1000 km of the atmosphere. Therefore, accurate measurements of Uranus' gravitational moments and magnetic field are necessary to reconcile these discrepancies and to further constrain models of Uranus' dynamo processes and interior dynamics.

Finally, while the existence of Uranus' intrinsic magnetic field suggests a warm interior driving convection, the equilibrium and effective temperatures of the planet are nearly equal [15]. This implies that parts of the deep atmosphere and interior of Uranus may not be convective, and the interior structure may be more complicated than a three-layer model [13, 51]. Further constraints on the interior structure and solid-to-gas ratio can inform our understanding of the formation of the solar system and solar systems containing ice giant planets [20].

2.2 Mission Goals and Objectives

For our mission concept we developed a focused, synergistic set of goals that would address the open questions outlined in the previous sections. The top-level goals of the QUEST mission concept and the respective science objectives are as follows:

- *Understand dynamos that drive magnetospheres in the solar system and beyond.*
    - ○ Distinguish between dynamo models for the generation of Uranus' magnetic field.
- *Identifying the energy transport mechanisms in Uranus' magnetic, atmospheric, and interior environments in contrast with the other giant planets*
    - ○ Investigate the prediction that Uranus' magnetosphere field opens and reconnects daily.
    - ○ Establish whether surficial winds and the banded structure of Uranus' upper atmosphere are related to deeper internal dynamics.
    - ○ Determine the explanation for Uranus' low thermal emission compared to Neptune and the other giant planets.

The QUEST science traceability matrix outlining our mission goals and objectives along with the measurement, instrument, and mission architecture requirements is provided in Table 1.

Table 1. The QUEST science traceability matrix: high-level science goals, specific science objectives along with the measurement requirements, instrument requirements, and mission architecture requirements to achieve the listed objectives. *Due to the limited scope of our study, investigation into the specific instrument operations required to achieve this objective was not fully explored (see Section 2.2.2) and would require further study for verification.

Science Goal	**Science Objectives**	**Scientific measurement requirement**		**Instrument**	**Instrument functional Requirements**		**Instrument performance**	**Mission requirements**
		Physical parameters	**Observables**		**Function**	**Requirement**		
Understanding dynamos that drive magnetospheres in the solar system and beyond	Distinguish between dynamo models for generation of the magnetic field	Magnetic field vectors and components	Magnetic field direction (20 mrad) and magnitude (0.1% of magnetic field) every 400 meters	Magnetometer	Range	+/- 20,000 nT	+/- 30,000 nT	Multiple orbits with periapsis ≤ 1.1 R_U.
					Resolution	0.1 nT	0.05 nT	
					Sampling rate	50 vectors/sec	100 vectors/sec	
		Electromagnetic perturbation	Radio emissions and plasma waves from open magnetic field regions	Plasma Wave Receiver	Frequency range	10 Hz to 5 MHz	1 Hz to 16 MHz	Multiple orbits with periapsis ≤ 1.1 R_U.
					Frequency resolution	5% ($\Delta f/f$)	1% ($\Delta f/f$)	
					Temporal resolution	4 s (Δt)	4 s (Δt)	
		Location of convective cells as a function of latitude and longitude	Brightness temperature	Microwave Radiometer	Inversion temperature precision	10 K	1 K	Multiple orbits with periapsis ≤ 1.1 R_U. Latitudinal coverage. Take data at multiple emission angles.
					IFOV	27°	20°	
Identifying the energy transport mechanisms in Uranus' magnetic, atmospheric, and interior environments in contrast with the other giant planets	Investigate the prediction that Uranus' magnetosphere opens and reconnects daily*	Magnetic field vectors and components as a function of time	Magnetic field direction (0.5°) and magnitude 10 nT	Magnetometer	Range	+/- 20,000 nT	+/- 30,000 nT	Multiple orbits with periapsis ≤ 1.1 R_U and measurements at distances > 18 R_U.
					Resolution	0.1 nT	0.05 nT	
					Sampling rate	50 vectors/sec	100 vectors/sec	
		Electromagnetic perturbation	Whistler waves associated with magnetic reconnection	Plasma Wave Receiver	Frequency range	1 Hz to 1 kHz	1 Hz to 16 MHz	Multiple orbits at distances > 18 R_U.
					Frequency Resolution	5% ($\Delta f/f$)	1% ($\Delta f/f$)	
					Temporal Resolution	4 s (Δt)	4 s (Δt)	

Establish whether surficial winds and banded structure of Uranus' upper atmosphere are related to deeper internal dynamics.	NH_3 and H_2S, gas volume mixing ratios as functions of depth and latitude	Brightness temperature as a function of emission angle (30° range) and latitude	Microwave Radiometer	IFOV	27°	10° to 20°	Need latitudinal and emission angle coverage. S/C spin along line of longitude, polar orbit.
				Integration time	100 ms	100 ms	
				Inversion temperature precision	Model input required	1 K	
	Cloud structure in the upper atmosphere	Visible images of high cloud features and images in 727 nm methane band	Wide-angle Camera	Spatial resolution	1000 km	300 to 600 km	Imaging away from periapsis
				Exposure time	3 ms	3 ms	
Determine the explanation for Uranus' low thermal emission compared with Neptune and the other giant planets.	Temperature profile of upper atmosphere (0.2 to 2000 mbar)	Ka-band and X-band amplitude and X-band frequency changes	High-gain Antenna	Frequency resolution	0.1 Hz	0.1 Hz	Occultation observation geometry
				Amplitude resolution	1000 ppm	100 ppm	
	Presence of a conductive layer in the atmosphere	Apparent deviation of atmospheric lapse rate (5 K)	Microwave Radiometer	Inversion temperature precision	2 K	1 K	Periapsis, radiometer facing planet every rotation. Spin along line of longitude, polar orbit.
	Distribution, depth, and relative concentration of NH_3 and H_2S, from 2 bar to ~200 bar	Brightness temperature as a function of emission angle and altitude down to 200 bar	Microwave Radiometer	Radiometer frequency	< 1 GHz	3 GHz to 600 MHz, 8 channels variable	Periapsis, radiometer facing planet every rotation. Spin along line of longitude, polar orbit.
				Inversion temperature accuracy	Model input required	0.1 %	

The QUEST mission concept goals and objectives directly address the two highest priority science objectives outlined in the 2013-2022 period NASA Planetary Sciences Decadal Survey [6] for a Uranus orbiter flagship class mission:

(1) *Determine the atmospheric zonal winds, composition and structure at high spatial resolution, as well as the temporal evolution of atmospheric dynamics,*

(2) *Understand the basic structure of the planet's magnetosphere as well as the high-order structure and temporal evolution of the planet's interior dynamo.*

In the following sections we expand on how the QUEST platform would allow us to address these high priority Decadal Survey goals as well as the goals and objectives specified in our science traceability matrix.

2.2.1 Dynamo Generation

The first major goal of the QUEST mission is to understand the dynamos that drive magnetospheres in the solar system and beyond. To achieve this goal, we aim to distinguish between dynamo models for the generation of Uranus' magnetic field (e.g., [52, 53, 54]) by (1) measuring the magnetic field magnitude and direction, (2) placing constraints on the global magnetic field configuration, and (3) determining the depth of convective cells as a function of latitude and longitude. The magnetometer would measure the magnetic field strength and direction during the 9 primary mission orbits, and the Plasma Wave Receiver (PWR) would identify the open field line regions from radio emissions and measure electromagnetic fluctuations produced by charged particles captured in the local magnetic field. The PWR would therefore provide information on the global magnetic field configuration (i.e., open vs. closed) while allowing for the separation of the magnetic field produced by the interior dynamo from those of the charged particles. The Juno mission resolved Jupiter's internal field to spherical harmonic degree 10 after 9 orbits [35] and we anticipate a similar resolution with our primary mission. Spherical harmonics to degree 10 would be sufficient to distinguish the contributions from the interior dynamo and the external perturbation resulting from, e.g., the solar wind interaction, and determine the interior dynamo depth at Uranus as well as the convective cell locations [53]. Therefore, the spherical harmonics information of Uranus would provide constraints on the theoretical predictions from different dynamo models and rule out inaccurate ones.

The Microwave Radiometer (MWR) would also provide measurements of abundances of condensable species in Uranus's atmosphere including ammonia and hydrogen sulfide. As a function of depth and latitude these measurements would constrain meridional circulation, and the overall abundance of ammonia at depths measurable by the MWR (200 bar) could confirm and measure the localization of the ammonia depletion observed by ground-based measurements [55, 56]. This ammonia depletion is hypothesized to relate to the presence of an ionic ocean at hundreds of kilobars [57, 22], which would constrain models that attempt to explain the magnetic dynamo of Uranus [14, 54].

2.2.2 Energy Transport in Uranus' Magnetosphere, Atmosphere, and Interior

The second major goal of the QUEST mission is to identify the energy transport mechanisms in Uranus' magnetic, atmospheric, and interior environments in contrast to the other giant planets. To investigate the energy transport mechanisms within Uranus' magnetic environment (i.e., the magnetosphere) we aim to investigate the prediction that Uranus' magnetosphere opens and closes daily [38]. Magnetic reconnection is a fundamental process that occurs in magnetized plasmas throughout the solar system and involves the conversion of magnetic energy into kinetic particle energy [58]. This energy conversion is due to a topological rearrangement of the magnetic field. Magnetic reconnection has been widely recognized to play an important role in energy transport throughout planetary magnetospheres [59] and has been observed at Mercury [60], Earth [61], Jupiter [62], Saturn [63] and Uranus [64]. Specifically, at a planetary magnetopause, magnetic reconnection occurs where the interplanetary magnetic field reconnects with the planetary magnetic field to form open field lines with one end fixed to the planet and the other open to the solar wind, such that the solar wind charged particles can enter the planetary magnetosphere. Meanwhile, open field lines are dragged anti-sunward by the flow of the solar wind, where they eventually reconnect again and the resulting newly-closed field lines travel back to the dayside where the cycle repeats. This process is known as the Dungey cycle [65]. It is one of the two primary mechanisms that drive convection in a magnetosphere, the other being the rotation of the planet. The dominance of either of these processes determines the overall dynamics of each of the solar system's various magnetospheres.

By measuring the magnetic field vectors and components as a function of time, we can identify plasmoids [64] and determine the reconnection of magnetic field lines with the aid of reconnection-associated Whistler wave measurements [66]. Additionally, the magnetic reconnection rate could be measured by dividing the normal

component of the magnetic field at the magnetopause (B_N) by the magnetic field at the magnetopause (B_{MP}). If no magnetic reconnection is occurring, the field lines at the magnetopause would be closed and there would be no normal component to the field. However, if magnetic reconnection is occurring, there would be a magnetic field component normal to the magnetopause magnetic field and by taking the ratio of these magnetic field measurements (B_N/B_{MP}) we could obtain a dimensionless rate of magnetic reconnection widely used in studies of planetary magnetic reconnection as was done, e.g., in the MESSENGER mission [67].

Due to the time-limited nature of our study, the instrument operations of our magnetometer and plasma wave instrument are not currently reflective of what is needed to identify reconnection events with confidence, though potential detections could be possible. Our study limits plasma wave receiver measurements to within 12 R_U (measured from Uranus' center) and high frequency (1/s) magnetometer measurements to within 2 R_U with low frequency (1/100s) for the remainder of the orbit. The whistler waves associated with magnetic reconnection would need to be measured with the plasma wave receiver near the magnetopause at ~18 R_U, and high frequency magnetometer measurements beyond 18 R_U are required to identify plasmoids produced by reconnection events. Further investigation is needed to determine the effect of these increased instrument operations on command & data handling and power consumption. It is also worth investigating the impact of replacing the plasma wave receiver instrument with a plasma spectrometer instrument. A plasma spectrometer would be capable of measuring electron and ion kinetic energy associated with magnetic reconnection and could be used in conjunction with magnetometer plasmoid detections to identify reconnection events as was done, e.g., in the Venus Express mission [68] and could impose less power and data requirements compared to a plasma wave instrument.

To further compare Uranus to other giant planets, we would establish whether surficial winds and the banded structure of Uranus' upper atmosphere are related to deeper internal dynamics by measuring the distribution, depth, and concentration of NH_3 and H_2S, and searching for indications of the presence of H_2O. The Juno spacecraft at Jupiter used its microwave radiometer to discover distinctive distributions of ammonia gas that varied with depth and latitude. This distribution of ammonia is indicative of some dynamics taking place at depth and pointed to "a Hadley cell without rain" [26]. Similarly, at Uranus, determining the concentrations of NH_3 and/or H_2S around ~5 bar with the 3 cm MWR band and at deeper levels in the atmosphere (down to 200 bar) within the 10-50 cm MWR spectrometer band would aid in comparing upper atmosphere dynamics to potential deeper dynamics. Additionally,

we would observe the cloud structure and height in the upper atmosphere using WAC visible images of high cloud features and images in the 727 nm methane band, which would allow for the calculation of atmospheric winds.

Lastly, we would investigate the origin of the low thermal emission of Uranus relative to Neptune and the gas giants. Measuring the temperature profile of the upper troposphere and lower stratosphere through radio occultations would constrain the heat flux through the upper layers of the atmosphere. Additionally, we would determine the presence of a conductive layer in the atmosphere by analyzing the MWR-measured spectrum from 10-50 cm. These MWR data would potentially provide insight into the existence of compositional gradients and conducting layers that inhibit heat flow. If there are no compositional gradients or conducting layers, this would indicate that the models for the lower atmosphere are incorrect [29]. The distribution, depth, and relative concentration of NH_3 and H_2S down to 200 bar would allow for testing of equilibrium models of the upper atmosphere [69].

3. Science Instrumentation

The instrument suite proposed for our mission concept was driven by the mission science goals and objectives as described in Table 1 and each instrument is based extensively on flight-proven designs. The instrument suite consists of five science instruments: a magnetometer, microwave radiometer, plasma wave receiver, wide angle camera with a methane filter, and a high gain radio antenna. The mass, power, data rate, and heritage information for each of these instruments is provided in Table 2.

The magnetometer, MAGnetometer investigations of an ICe giant (MAGIC), would measure Uranus' magnetic field magnitude and orientation. The MIcRowave RadiOmeteR (MIRROR) would probe the deep atmosphere by providing data on gas volume mixing ratios as a function of depth and latitude and any patterns indicative of global circulation. The plasma wave receiver, Plasma-wave Receiver Exposing Structure of The dynamO (PRESTO), would provide information on thermal plasma, dust, and lightning based on the electric and magnetic fields measurements. Additionally, PRESTO would aid in interpreting the magnetic field data obtained by MAGIC through the removal of confounding signals produced by plasma waves. The Wide-Angle methaNe Detector (WAND) would investigate the upper atmosphere, providing a probe of cloud height in the upper troposphere and estimations of wind speeds through cloud tracking. The high gain communications antenna and associated transmitter/receiver hardware, RadiAnt, would be used for radio science experiments. Radio occultations

and gravity field measurements would provide further data on the atmospheric and interior structure of Uranus. Each of these proposed instruments and their capabilities are discussed in further detail in the following subsections.

Table 2. QUEST instrument suite mass, power, data rate, and heritage information.

Instrument	Mass (kg)	Power (W)[1]	Data per orbit (Mb)[2]	Heritage
MAGIC (magnetometer)	1.5	4	18	MAG (Juno)
PRESTO (plasma wave receiver)	6	6	3780	Waves (Juno), RPWS (Cassini)
MIRROR (microwave radiometer)	42	33	356.4	MWR (Juno)*
RadiAnt (radio antenna)	14.4	80.7[3]	N/A	New Horizons, Cassini
WAND (wide-angle camera)	10.5	7	2400	MVIC (New Horizons), JunoCam (Juno)*

[1]Listed values are average power unless otherwise noted.
[2]Listed values are data per science orbit in megabits, uncompressed
[3]Peak power
*instrument is significantly modified from heritage design

3.1 MAGIC (Magnetometer)

MAGIC would measure the magnitude and direction of the magnetic field as the QUEST spacecraft orbits Uranus. During the various phases of the insertion and science orbits, the dynamic range of MAGIC could be modified to obtain data at appropriate resolutions. MAGIC would be capable of measuring a maximum field strength of +/- 30,000 nT at highest dynamic range, which is well within the maximum observed field strength during the Voyager 2 flyby (413 nT) providing substantial headroom for greater field strength [14]. The magnetometer instrument is based on the Juno magnetometer instrument with two magnetometers mounted on the boom in a gradiometer configuration for magnetic cleanliness. At its most sensitive, MAGIC could sample the vector magnetic field with a resolution of 0.05 nT, which is comparable to other flight-tested magnetometry experiments [70]. MAGIC would be operated at the maximum sampling rate of 100 vectors/second, producing 1.6 kbits/second, within three hours of each periapse pass at 1.1 R_U, and at a background data rate of 1 vector per 100

seconds for the rest of each orbit, producing a total of about 18 megabits of data per orbit. All MAGIC data would be transmitted to Earth uncompressed. Nine periapse passes are planned during the primary mission, ensuring substantial longitudinal and latitudinal coverage for magnetic field measurements. The Juno mission was capable of achieving a degree 10 spherical harmonic model of the magnetic field at Jupiter after 9 orbits [35]. Our mission architecture aims to mirror Juno, and so we anticipate the data products from the Uranus magnetic field investigation could be used to constrain models of dynamo generation and fit magnetic field models to harmonic degree of order 10 within our nominal 9 orbit mission. With the aforementioned specifications, MAGIC would meet the objective of collecting sufficient data to significantly improve our understanding of Uranus' magnetic field environment.

3.2 PRESTO (Plasma Wave Receiver)

PRESTO would be used to monitor the radio emissions from Uranus' magnetosphere and measure the plasma waves inside Uranus' magnetosphere. The diversity of the emissions detected by Voyager 2 during its brief flyby was unprecedented, and some observed phenomena still lack sufficient explanation [71, 72]. Voyager 2 observed intense radio signals before closest approach at 58.8, 78.0, and 97.2 kHz, and similar radio emissions were also detected up to much higher frequencies (~800 kHz) by the planetary radio astronomy experiment [73]. Meanwhile, the plasma wave measurements by Voyager 2 demonstrated that intense plasma wave activity developed only in the inner magnetosphere ($r < 12\ R_U$); this result is similar to that found at Saturn [74, 75]. Uranus' inner magnetosphere is characterized by strong whistler-mode emissions that occur below the electron cyclotron frequency ($f_{ce} = 28|B|$, where $|B|$ is measured in nT, and f_{ce} is measured in Hz, and thus $f_{ce} \sim 644$ kHz). Since the maximum plasma frequency of the dayside ionosphere is typically about 5 MHz, we have selected 16 MHz as the upper frequency limit for the electric field measurements [76]. During the QUEST science orbits, PRESTO would be able to further monitor the complicated emission spectrum from within the magnetosphere, surveying over multiple Uranus days (requiring PRESTO operation through a minimum of 3 orbits). PRESTO would offer further insight into the nature of the correlation between solar wind activity and wave phenomenon within the magnetosphere, determine the plasma density in the magnetosphere of Uranus, and shed further light on the dynamics of the most complex planetary magnetosphere in our solar system. In addition to the PRESTO primary science observations, low frequency measurements of the electric and magnetic fields could be used to remove confounding source observations from the data obtained by the MAGIC experiment. Therefore, given that MAGIC

would be operated for 9 orbits to obtain the highest degree spherical harmonic model, PRESTO would operate during 9 orbits as well.

PRESTO would take advantage of the heritage afforded by the Cassini Radio and Plasma Wave Science (RPWS) investigation (i.e., the antennae, frequency receivers, data processing unit, waveform capture procedure) [76]; the only modification includes shifted frequencies to account for differences between the Uranian and Saturnian magnetic environments. A coil antenna is used to make single axis magnetic field measurements, and electric field measurements are made with a 5-meter V configuration dipole. As with Juno, the spin of the QUEST spacecraft creates an effective second axis for the electric field measurement. PRESTO would be sensitive to electric and magnetic fields from 1 Hz - 12 kHz, and the electric field could additionally be measured up to 16 MHz [76]. The frequency (~ 5% ($\Delta f/f$)) and temporal (~ 4 s/sweep) resolution of PRESTO would be limited by the sampling time, which would be at a maximum closer to periapse. Background data rate for PRESTO is expected to be around 1 kbit/s, increasing to 1 mbit/s during the periapse pass, for a combined total of 3.78 Gbit of data per orbit. These data rates are conservative estimates based on the upper end of Cassini RWPS design data volumes. PRESTO data would be compressed using a lossy algorithm for initial transmission during the 9 initial orbits, and a lossless version of the data may be transmitted subsequently (Section 4.3.4).

3.3 MIRROR (Microwave Radiometer)

To probe Uranus' atmosphere at depth, we would use QUEST's MIcRowave RadIometeR (MIRROR) instrument. MIRROR's capabilities would allow it to collect data which, besides contributing to each of QUEST's major science goals, would provide a highly valuable complement for datasets obtained by missions at other giant planets and for decades of ground-based observations. By sensing particular regions of Uranus' atmosphere at multiple emission angles, we would be able to probe the abundances of ammonia and hydrogen sulfide as a function of latitude and depth; better understand what processes contribute to the generation of Uranus' unique magnetic field; search for the source of Uranus' anomalously low heat output; and test the theory of Uranus' deep supercritical layer of water. The observed brightness temperature as a function of altitude and emission angle provided by MIRROR would also aid in the determination of the depth, stability, and structure of the banded atmosphere.

MIRROR would work by measuring brightness temperature, a characteristic that is dependent on both the pressure/temperature profile and local opacity sources [77, 78]. By assuming the deep temperature profile of Uranus

follows an adiabat (which is routine for other gas giants) the opacity of the atmosphere at different pressure levels could be derived uniquely from the measured brightness temperature. Through knowledge of the absorption efficiency of Uranus' atmospheric gases (especially ammonia and hydrogen sulfide), by using thermochemical equilibrium models to predict the location of clouds and opaque gas species throughout the troposphere [69], and by measuring pressures above and below the predicted locations of such clouds (especially the predicted ammonium hydrosulfide cloud at ~20 bar), we could retrieve the abundance of a gas whose opacity affects the output brightness temperature [77, 79].

MIRROR's channels were selected to probe those particular layers of the atmosphere that would help resolve outstanding questions not only for the Uranian atmosphere but for the system as a whole. Channel 1 would be centered on 2 cm (15 GHz), integrating over a 500 MHz bandwidth with a ~500-km footprint on the planet at closest approach, and would sound the atmosphere to a depth near 5-10 bar. This channel would provide further context and validation for decades of ground-based observations (including those made at the Very Large Array and other radio telescopes) by providing unprecedented spatial resolution as well as different viewing geometries at depth over the course of QUEST's orbit. Channel 1 would also be able to probe the region well above the theorized ammonium hydrosulfide cloud layer at ~20 bar. Depending on the relative amounts of ammonia and hydrogen sulfide in Uranus' atmosphere, one of these gas species will dominate the 5-10 bar region after combining to form the ammonium hydrosulfide cloud. Current observations point to the dominance of hydrogen sulfide gas in this part of the atmosphere and a hydrogen sulfide cloud within 3-5 bar [81, 82], and Channel 1 could further confirm (or challenge) these recent deductions. The dominance of hydrogen sulfide could also allow MIRROR to indirectly probe the supercritical water layer, as a hydrogen sulfide cloud at 3 to 5 bar would be indicative of ammonia being readily dissolved in the water layer and consequently depleted elsewhere in the atmosphere [57].

Channel 2 would cover a much wider bandwidth than Channel 1, from 10 to 50 cm or 3 GHz to 600 MHz, with a ~530-900-km footprint on the planet at closest approach and sounding depths of the atmosphere from 20-200 bar. Channel 2 would comprise a single large (nominally 1.6 m x 1.6 m) patch array antenna to enable the low-frequency 600 MHz sounding, but would host improved receiver electronics including an 8-channel digitizer able to spectrally divide the 600 MHz to 3 GHz antenna bandwidth into eight separate simultaneously-measurable portions [83, 84]. These discrete spectral channels, as opposed to integrating over the entire band, would allow for inter-orbit dynamic bandwidth shifts for SNR optimization at different levels of the atmosphere following a first-orbit

measurement. This digitizer allows for, essentially, the separation of Channel 2 into several other discrete channels, thereby creating a measurement analogous to Juno's few lowest channels and allowing for better differentiation of the spatial distribution of opaque gas species in the deep atmosphere. The relatively quiescent radiation and synchrotron flux near Uranus compared to Jupiter would allow for a more straight-forward antenna design than Juno's MWR patch array antennas [85]. In this region of the atmosphere, Channel 2 would be sensitive to the combined opacity from both ammonia and hydrogen sulfide. Since ammonia and hydrogen sulfide combine in equal parts to condense into an ammonium hydrogen sulfide cloud, knowing the hydrogen sulfide abundance in the region of the atmosphere as measured by Channel 1 would allow for the extraction of the ammonia abundance at these depths.

Using Juno's orbital pattern as an example and its microwave radiometer as a legacy instrument, the QUEST orbital geometry and spacecraft rotation would enable measurements of the emission-angle dependence of these opacity sources, allowing us to understand the spatial structure of these opacity sources at depth [88]. At a spin rate of 3 rpm, the 100 ms integration time of MIRROR would allow for measurements at 1.8° intervals, which is less than 1/10 of the beam size for the largest beam width. The beam width parameters were based on achievable values of the MWR on Juno as well as the desire to sample the atmosphere at a resolution of 2° in latitude during periapse. This would also be supported by laboratory experiments of the microwave absorption properties of the main condensable species (ammonia, hydrogen sulfide, water), as was done prior to the Juno mission [79].

While a single orbit of MIRROR data would be sufficient to measure the distribution of opaque species in Uranus' atmosphere along a single line of longitude, being able to compare changes in brightness temperature across multiple longitudes would provide valuable insight into patterns of circulation and temperature profile deviations in Uranus' deep atmosphere. The 5 planned orbits dedicated to MIRROR observations would be sufficient to examine differences or similarities between different regions of the planet and better understand how they compare to those seen at Jupiter (MWR data from Juno's first 14 perijove passes have shown a deep ammonia abundance that is remarkably consistent across longitude [80]). While the planned MIRROR orbits are sufficient to achieve our science goals, further orbits in an extended mission can always bolster the statistical significance of any patterns observed in the deep atmosphere.

Each 16-bit channel, with a 10-ms sampling rate, would obtain 160 bits of data every second. Over the course of one sampling period (the 40-minute periapse and 3-hour sky-viewing), a single 16-bit channel would

acquire 39.6 Mbit/orbit. Channel 1 is a single 16-bit channel, but Channel 2 is comprised of 8 16-bit channels due to the 8-channel digitizer. Assuming all 9 16-bit channels are collecting data, we would obtain 356.4 Mbit/orbit and therefore 5 MIRROR-oriented orbits would allow us to collect a total of 1782 Mbit.

Combined, these two channels would provide information on the vertical distribution of opaque gas species at depth as a function of latitude. It is important to note here that computing the precise contribution functions of MIRROR's channels and the exact ability of these different emission angle measurements to measure the spatial distribution of opaque species at the depths mentioned here requires further investigations that are beyond the scope and ability of this study; however, we are confident that we would be able to measure opacity as a function of emission angle at different depths, and this would enable us to achieve our science goals as related to MIRROR. Juno's Microwave Radiometer discovered ammonia gas distributions that were anything but uniform; they were indicative of large-scale circulation in the deep atmosphere [26]. Similarly, MIRROR would be able to observe changes in opacity that could be used to constrain dynamical atmospheric models.

Thus, our multi-channel radiometer would enable the study of upper atmospheric dynamics (Channel 1) that would add crucial context to current and future ground- and space-based measurements, and also offer a unique glimpse into the deep atmosphere (Channel 2) to answer fundamental questions about the potential supercritical layers below. Such measurements of the water abundance are critical for differentiating between formation theories for the ice giants [86].

3.4 RadiAnt (Radio Antenna)

QUEST would use its Radio Science Antenna (RadiAnt) to transmit and receive radio signals to and from Earth. This instrument would contribute minimal additional mass, power, and cost, because it capitalizes on equipment and radio signals already required for telecommunications with Earth. The received amplitude, phase, and Doppler shift associated with these communication signals could be used to obtain ionospheric electron density and atmospheric temperature, pressure, and density profiles as well as measurements of the gravitational moments of Uranus resulting from an unequal distribution of mass across the planet [87]. The baseline technology for this instrument is the Voyager 2 radio antenna, which acquired data on Uranus' atmosphere from 0.3 mbar to 2 bars over an altitude of approximately 250 km and latitude range of 5 degrees. The data allowed for a temperature model with an uncertainty ranging from 10 K at 0.5 mbar to 2 K at 2 bar if the uncertainty in composition is assumed negligible.

This heritage instrument achieved a frequency resolution of approximately 0.1 Hz and amplitude change resolution of 100 parts per million [77]. During atmospheric occultation of the spacecraft, the refraction and attenuation of the signal could be used to deduce the upper atmospheric temperature profile. The QUEST platform would provide four occultation opportunities allowing for improved latitudinal coverage over the Voyager 2 flyby. Additionally, as the spacecraft would enter the gravitational field of the planet, the Doppler shift of its radio transmissions could be analyzed to obtain up to J6 gravity moments with reasonable uncertainties, thus providing verification and improvements upon Voyager 2 gravity measurements. No data downlink burden is associated with RadiAnt, because measurements are conducted on Earth rather than at the spacecraft.

3.5 WAND (WAC)

WAND is proposed to be a visible light camera that derives its heritage from the JunoCam aboard the Juno Jupiter orbiter [89]. The camera would have a 1 rad field of view (FOV), a 0.672 mrad Instantaneous Field of View (IFOV), and four filters, including three for visible light (R: 600-800 nm; G: 500-600 nm; B: 420-520 nm) and one methane band (band center 725 nm with a 25 nm FWHM). The camera would be mounted on the bottom of the hexagonal bus. Because the spacecraft is spinning, time-delayed-integration (TDI) is employed to shift images one row over a short period during the exposure to account for scene motion due to the spacecraft's rotation.

WAND would be used to fulfill one primary science objective and four secondary, opportunistic objectives, as well as imaging for public outreach. The notional primary objective is monitoring cloud formation, structure, height, and motion with approximately monthly frequency. Opportunistic secondary science objectives include (1) images of upper atmosphere structure at spatial resolutions of up to 36 km at closest approach; (2) images of the northern hemispheres of major satellites and rings at resolutions of 2 to 7 km; (3) survey for additional small satellites within the ring system. WAND would produce 6 four-channel images at 100 megabits per channel on each of the 9 science orbits (see Section 4.3.4 for data transmission details).

3.6 Opportunistic Measurements

There are several opportunities for QUEST to make observations of the Uranian system that can address additional outstanding questions. These observations are opportunistic and not a part of the baseline science goals for the mission, but they would provide further information about Uranus' mysterious moons, rings, and atmosphere.

While the primary purpose of WAND, the Wide-Angle Camera (WAC), would be to image Uranus' atmosphere, it could also be used to examine Uranus' satellites and rings. Deducing the surface features and color of

Uranus' moons, especially those with evidence of surface activity [90] would provide valuable insights into the evolution of the Uranian system. The resolution of the images we would potentially be able to obtain is on the order of kilometers/pixel which would only improve on Voyager 2 images because a different area of the satellite would be imaged. Additionally, imaging Uranus' rings at various viewing geometries and phase angles would help constrain the size of ring particles, their ages, and their origins. The plasma wave receiver, PRESTO, could also aid in determining dust concentrations in ring plane crossings [76].

Due to QUEST's orbit, there would also be several opportunities to take advantage of the visibility of the dark side of the planet. Jupiter's aurorae were observed by Galileo's Solid-State Imaging camera in the visible wavelength regime [91], and while Uranus' aurorae are not well understood, the possibility to image them on the nightside of the planet remains. WAND could also capture lightning on the dark side of the planet, providing information about moist convection in Uranus' atmosphere.

Even though we did not study these opportunistic measurements in detail, they could add further science value to our primary objectives but would not be focused on in order to reduce mission complexity and cost. In our study, we found that our primary objectives could be achieved at a significantly reduced cost compared to a flagship class mission through careful selection of a synergistic instrument suite. In the following sections, we describe our mission concept designed to achieve these goals including the instrument suite, spacecraft design, launch profile, and the associated cost, risk, and schedule.

4. Mission and Spacecraft Design

The following subsections outline the mission architecture, launch vehicle, launch trajectory, orbital parameters, notional spacecraft design including configuration, propulsion and attitude control, power and thermal management, command and data handling, and communications and science operations schedule proposed to achieve the QUEST mission science goals and objectives.

4.1 Launch Vehicle Trajectory

The overarching objective of the mission design for the concept study was to maximize the delivered mass into Uranus orbit within the top-level constraints imposed by the New Frontiers 4 AO. The large heliocentric distance to Uranus (19.2 AU) results in time of flight no shorter than 10 years even using the Atlas V551 launch vehicle which was the most capable available for New Frontiers missions. Use of a Solar Electric Propulsion (SEP)

stage to shorten the time of flight was not a feasible option due to mass and cost restraints. Aerocapture, which could shorten the flight time and increase delivered mass at Uranus by reducing the spacecraft's approach velocity via atmospheric drag, was also not considered due to an insufficient technological maturation level, i.e. could not feasibly be brought to TRL 6 by Preliminary Design Review (PDR), for use on a New Frontiers mission, which tends to rely on high heritage mission critical technologies. Additionally, study ground rules required a launch no later than December 31, 2032. There was a 15-year maximum flight time constraint because the radioisotope power system (RPS) had a design life of 17 years, and to allow at least 2 years of science operations the transit time must not exceed 15 years. The mission design we would implement, ~13 year flight time and ~1 year of science operations (see below and Section 4.2), leaves plenty of margin for the RPS power to reduce risk, allow for flexibility in operations and the potential for an extended mission. We chose an orbiter for our mission architecture because our selected science objectives require long duration, extensive spatial coverage measurements that are not possible with a flyby architecture.

Based on these top-level requirements, the mission design team evaluated ~100 potential gravity assist trajectories from a broad search program, which were originally compiled for the NASA Ice Giants Pre-Decadal Study [8]. Based on this survey, several trajectories to Uranus launching in May 2031 and July 2032 were found to maximize delivered mass as the launch timing allowed a Jupiter gravity assist. These trajectories and a few backup trajectories were analyzed using higher fidelity tools, custom to JPL and Team X, to obtain more accurate estimates of their performance. We ultimately selected an Earth-Deep Space Maneuver-Earth-Jupiter-Uranus trajectory launching in May 2032 and arriving at Uranus in May 2045 after a 13-year flight time. The availability of a Jupiter gravity assist is enabling for a Uranus New Frontiers mission because in the time frame when a Jupiter gravity assist is unavailable the deliverable mass drops significantly, as shown in Figure 6. While past flagship mission concept studies [e.g., 8] have used a Jupiter gravity assist to get more mass into orbit around Uranus, this trajectory window has not been used prior to this study for a New Frontiers class mission. The smaller budget for a New Frontiers mission limits the spacecraft mass even more strictly (compared to a more expensive flagship) and thus the gravity assist becomes even more critical for getting a spacecraft with multiple instruments into orbit around Uranus [e.g., 10]. For example, a previous Uranus mission concept study that did not utilize the Jupiter gravity assist, OCEANUS [10], had to rely on Solar Electric Propulsion (SEP) and therefore was only able to carry one non-donated scientific instrument, a magnetometer, in order to stay within the cost cap.

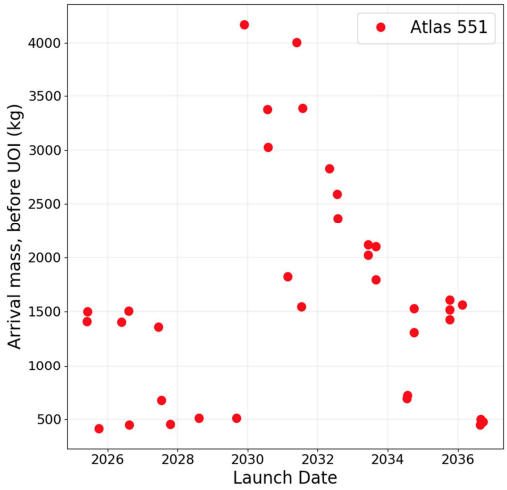

Figure 6. Arrival mass values for launch windows between 2025 and 2037 using the Atlas V551 launch vehicle. A Jupiter gravity assist available between 2030 - 2032 launch dates yield a significant increase in deliverable mass.

We chose the Atlas V551 as our launch vehicle because it was the most capable option to maximize the delivered mass. We found that maintaining healthy mass margins was a significant challenge because the large heliocentric distance and desire to minimize flight time results in high orbit insertion ΔV (change in velocity of spacecraft), which means a significant portion of the mass is allocated to propellant for the orbit insertion maneuver. However, the selected trajectory satisfied all the study ground rules and constraints and delivered sufficient mass into Uranus orbit to perform the QUEST science mission. Figure 7 shows the key events and dates for the selected trajectory. The proposed trajectory has a launch C3 of 28.96 km^2/s^2 and an arrival V_∞ of 5.96 km/s. V_∞ refers to the speed of the trajectory with respect to a target and C3 refers to the characteristic energy, equal to the earth departure V_∞^2. The declinations of the launch asymptote and the arrival asymptote are -15.94 degrees and -49.69 degrees, respectively.

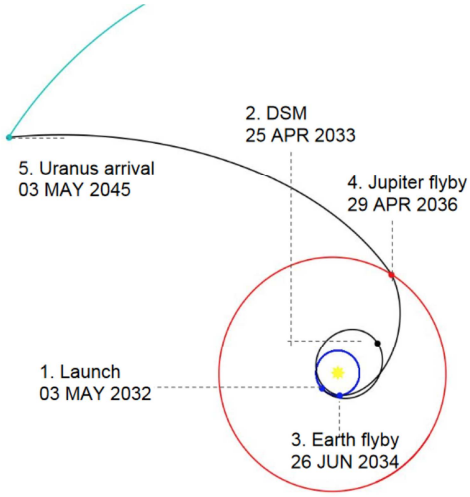

Figure 7. 13-year E0EJU trajectory selected for the mission concept (0 indicates DSM).

4.2 Orbit Design

The proposed high priority science investigations of the magnetic field and atmosphere preferred a high inclination, polar orbit which offers extensive latitudinal and longitudinal coverage similar to Juno's orbit at Jupiter. If multiple close flybys of the Uranian moons were desired, a near-equatorial low inclination orbit would need to be selected. However, moon science was deemed a low priority objective in this study and drove the selection of a high inclination, near polar orbit. The selected inclination was ~80 degrees, though a near 90-degree orbit was desired by the magnetic field investigation science team. The quoted inclination is with respect to Uranus equator, and was driven by constraints emanating from ring plane crossing hazard. The orbit periapsis of 1.1 R_U lies within the rings, so the inclination was chosen such that the node crossings fell in designated gaps within the ring plane deemed safe by the risk and programmatics. Ultimately, the ~80-degree orbit satisfied the ring plane safety constraints over the mission duration and was acceptable while the 90-degree inclination was deemed unsafe.

The orbital period selection is a trade-off between science requirements and engineering constraints. Some science requirements preferred a low Uranus circular orbit at 1.1 R_U, inside the innermost rings. However, the ΔV cost to achieve this circular orbit would be prohibitive, and so the team considered a high elliptical orbit (~180 days period) with a low periapsis (1.1 R_U). However, the 180 days orbit would be too long for the limited duration of the mission and the spacecraft would not achieve sufficient latitude and longitude coverage during the periapsis pass to accomplish the science objectives. The ring plane crossing hazard was also a concern for a low periapsis orbit.

The compromise was to capture into an initial 100-day orbit with a 1.1 R_U periapsis to minimize orbit insertion ΔV. Analysis performed by our perceived risk and mitigation strategy team (outlined in section 5.3) indicated that our selected periapsis altitude would be sufficient to mitigate the hazard of dangerous particle collisions with our spacecraft during ring plane crossings. At the end of the first capture orbit, the spacecraft would perform a Period Reduction Maneuver (PRM) to lower the period to 30 days. The apoapsis radius for the 30-day operational orbit is about 76 R_U. The angle between the orbital plane and noon local time plane is approximately 24 degrees. A spinning spacecraft bus would be employed (as opposed to 3-axis stabilized) to reduce the fuel required for microwave radiometer scanning procedures and to provide an extra effective dimension for monitoring low frequency waves by the plasma wave receiver as well as providing multiple emission angle measurements for MIRROR. This notional spinning spacecraft design additionally allows for limited radiometer data collection during radio science passes where the high-gain antenna is pointed towards Earth. The proposed prime mission of one year starting from arrival date at Uranus thus allows nine 30-day orbits with 1.1 R_U periapsis and was deemed acceptable for the science team to perform the investigations outlined in Table 1.

The primary mission would end one year after arrival, but the only major limiting constraint on extended operations is the radioisotope power source (RPS) degradation and on-board propellant. With a planned design life of 15 years for the RPS, this allows for at least one year of extended mission with no power restrictions. Further operation is likely possible, albeit with lower power available and the potential requirement for instrument cycling to compensate for the limited power output. At the end of the mission the spacecraft would be disposed of into Uranus to prevent the possibility of contaminating moons, some of which may harbor subsurface oceans or other habitable environments. De-orbit ΔV is accounted for in the mission design to comply with planetary protection policies.

4.3 Spacecraft Design

The notional design and configuration of the QUEST spacecraft (Figure 8) and its associated subsystems were carried out in cooperation with Team X, JPL's concurrent engineering mission design team. The resulting proposed mission architecture was selected based on its ability to achieve the specified science objectives while remaining within mass, power, and cost margins as specified by the New Frontiers 4 Announcement of Opportunity [5].

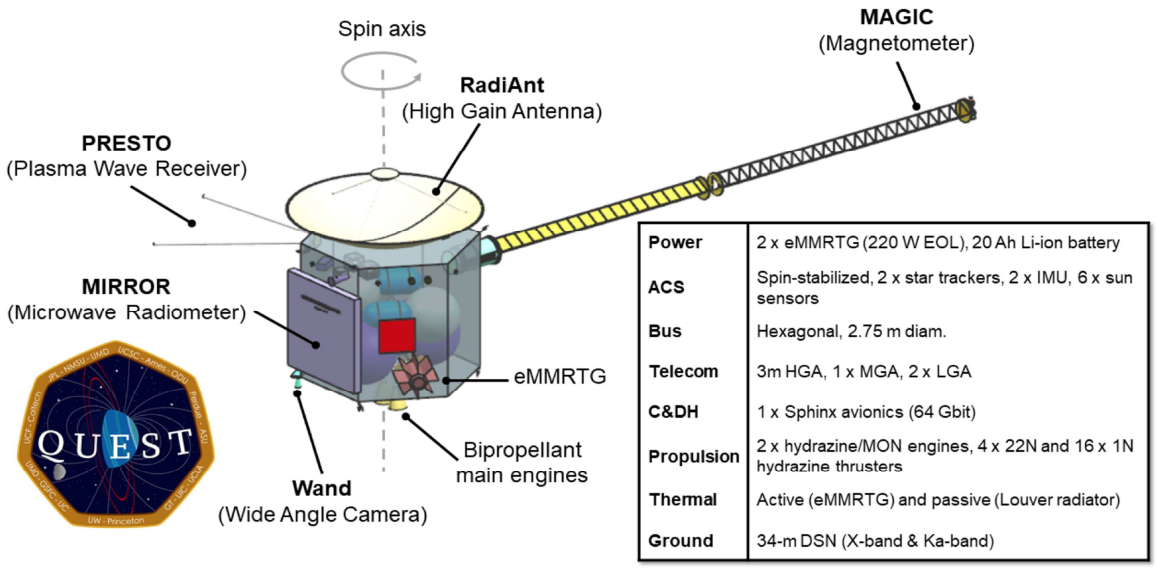

Figure 8. Baseline spacecraft schematic and summary table showing location of baseline instruments and spacecraft components.

4.3.1 Structure and Configuration

The potential science instruments and subsystems for the QUEST mission would be housed within a hexagonal bus with a 2.75 m circumscribed diameter and a maximum stowed width of 3.7 m, well within the capacity of the 5.4 m fairing of the Atlas V 551 launch vehicle. The spacecraft could also fit in the 4-meter fairing of the Atlas V 431, but the scope of our study was insufficient to explore the trades between these fairings. The bus would contain four fuel and oxidizer tanks thermally regulated by two Enhanced Multi-Mission Radioisotope Thermoelectric Generators (eMMRTGs) mounted on the outer panels. The MIRROR and PRESTO antennae would be body-mounted, and PRESTO's antennae would initially be stowed. MAGIC would sit on a composite boom that extends 10 meters beyond the bus once fully deployed, bringing QUEST's potential maximum deployed width to 12.5 m. The notional layout of the fuel tanks, science instruments, and various subsystem components is optimized to balance the total dry mass of 1210 kilograms evenly across the spacecraft.

4.3.2 Propulsion and Attitude Control System (ACS)

QUEST would use a dual-mode chemical bipropellant system to propel the spacecraft. It would consist of two bipropellant main engines for the deep space maneuver (DSM) and Uranus orbit insertion (UOI), four medium monopropellant thrusters for trajectory correction maneuvers, and 16 small monopropellant thrusters for fine attitude control. The thrusters are proposed to be arranged in orthogonal clusters at corners of the hexagonal spacecraft bus.

The interior of the bus would contain two hydrazine tanks, two nitrogen tetroxide tanks, and three helium pressurized tanks. The propulsion system would deliver the required UOI ΔV of 949.6 m/s, where it would reach a peak power requirement of 211 W. The proposed design makes use of off-the-shelf engines and tanks along with standard lines and valves, and the design maintains a 20% tank margin for propellant required for potential additional maneuvers. The ΔV budget is provided in Table 3.

Table 3. ΔV Budget.

Maneuver	ΔV (m/s)
DSM	647.4
DSM Biasing & Flyby Targeting	42.4
UOI	949.6
Period Reduction	83.2
Disposal	15
Total	**1737.6**

The attitude control system (ACS) would provide the positional and pointing accuracy necessary to conduct targeted science measurements and to accomplish required turning maneuvers. The ACS for the spin-stabilized spacecraft would consist of two star trackers, six sun sensors, and two inertial measurement units (IMUs). The sun sensors are included to provide spacecraft orientation information if the star trackers become misguided. Due to the hexagonal shape of the spacecraft bus, one sun sensor is included on each face. It was necessary for the QUEST ACS to be a spin stabilized system due to the requirements of the MIRROR instrument (multiple emission angles). Spin stabilization also removes the need for reaction wheels, which allows us to save on power and cost while avoiding the risk of reaction wheel failure.

During the proposed long cruise stage of the mission, the spacecraft would continually point the high-gain radio antenna X-band and Ka-band toward Earth. QUEST would use thrusters to continually ensure the spacecraft is pointed to within 0.5 degrees of the desired path to Uranus. The ACS also relies on the thrusters to maintain a spin rate of about 3 rpm and for spin up during initial orbital insertion. The pointing control would be 900 arcseconds (~120 km resolution at Uranus periapse), pointing knowledge would be 60 arcseconds, and pointing stability would be 60 arcseconds/second (~8 km resolution). After orbit insertion at Uranus, the spacecraft would perform

maneuvers to allow the MIRROR instrument to accomplish its associated science goals. Two maneuvers during each of the five MIRROR orbits would point the antenna back towards Earth after the necessary measurements are completed.

4.3.3 Power and Thermal Management

The design of the potential power system is constrained by the solar flux available at the distance of the Uranian system at 19 AU and the power requirements of the science instruments and spacecraft subsystems. A solar array-only power architecture (without a radioisotope heater unit (RHU) for electronic thermal regulation) was considered impractical because it would require over 200 m^2 of solar panel area, with an associated mass greater than 800 kg using current technologies. Recent developments in thermoelectric coupler (TEC) materials, the electronic component converting heat into electrical current, have enabled the potential development of enhanced multi-mission radioisotope thermoelectric generators (eMMRTG), with a power output 50% higher than current MMRTGs at the end of design life (EODL) [92]. Although this technology has not flown yet, it is a low-risk modification of the MMRTG design [92] and therefore could be expected to have the proper TRL during QUEST Phase A in the late 2020s.

Our design would require only two eMMRTGs with a 220 W total output at the end of mission (EOM), 14 years from ^{238}Pu fueling. With this setup, power balance would be positive during cruise, cruise approach science (CAS), orbital science, and safe mode. The inclusion of a single lithium-ion secondary battery of 20Ah is sufficient to accommodate peak power requirements in CAS + telecom, orbital science + telecom, deep space maneuver and Uranus Orbital Insertion modes, while being recharged during power positive orbital science mode. The proposed timing of each mode was tuned to allow sufficient recharging time during power positive periods. Our proposed design considers a 14% degradation of the battery after 14 years, and still provides a comfortable margin with at least 340 Wh altogether. The power control system electronics would have a dual-string design inherited from the Mars Science Laboratory rover, and the power system has an overall 43% margin in power generation.

The proposed thermal system is designed to maintain the internal electronics, propulsion module, propulsion lines, and thruster packs within operating temperatures throughout the mission. The spacecraft bus would be insulated with standard multi-layer insulation (MLI) and maintained in the temperature range of 253 - 323 K. The proposed bus, containing the propulsion module and electronics, would be actively heated from excess heat from the two eMMRTGs totaling 120 W and passively cooled via Louver-covered radiators that are sized to discard 320 W of

heat at UOI. The propellant lines and thruster packs would be maintained in the temperature range of 290 - 308 K via a 15 W electric heater and 42 1 W variable radioisotope heater units (VRHU), respectively.

4.3.4 Command and Data Handling

QUEST would use a dual-string command and data handling architecture built around the Sphinx avionics system [93]. The Sphinx avionics system coordinates data transfer between the science instruments and spacecraft subsystems, data storage, and science and telemetry data downlink. Because on-board storage cards are capable of storing 64 Gbit of data, the main limitation on the downlink of science data taken on orbit from the spacecraft to a 30-meter Deep Space Network (DSN) antenna is the downlink data rate and time per orbit. Both of these parameters would be limited by the distance of the spacecraft from the Earth and the availability of the DSN antenna for communication. Using Ka-Band downlink, the nominal downlink rate would be 6.4 kbit/sec, and the available DSN receiving time would be nominally 8 hours/day, giving a daily data downlink of 184 Mbit. QUEST would orbit Uranus with a 30-day period following insertion and capture orbit period reduction, and 8 of these days would be used for science data collection, leaving 22 days for data downlink. This would give a per orbit data downlink limit of 4.06 Gbit.

QUEST would produce 6.5 Gbit of raw science data per orbit, to be compressed using a combination of lossless and lossy compression to 3.5 Gbit (Table 4). The majority of this, ~5 Gbit raw, would be produced in the hour surrounding periapse. A complete data archive using only lossless compression for all 9 science orbits would be recorded in the Sphinx NAND flash memory, with 27.5 Gbit remaining (Table 5). The vast majority of QUEST data would be produced by PRESTO and WAND, so compression algorithms used on these datasets would be key. We would expect to achieve roughly 50% reduction in PRESTO data volume using entropy coding [94], and wavelet-based compression on WAND images. Compression would occur on the Sphinx FPGA, leaving the CPU unburdened and preventing downlink backlog between science orbits. The full lossless data archive would be downloaded subsequent to completion of the primary mission, and some raw data records of interest could be pulled each orbit once the lossy compressed records have been successfully downlinked.

Table 4. Per-orbit instrument data volumes.

Instrument	Data volume per orbit (raw, Mb)	Data volume per orbit (loss compression, Mb)
MAGIC	18	18
PRESTO	3780	1890
MIRROR	356.4	356.4
WAND	2400	1200
RadiAnt	N/A	N/A
Total	**6454.4**	**3464.4**

Table 5. Mission total data volumes.

Mission data volume (9 orbits)	Data (Mb)
Instruments, raw	57564
Instruments, compressed	29754
Available Ka-band downlink	36540
Available onboard storage (NAND flash)	64000

4.3.5 Communications

The proposed QUEST spacecraft is designed to carry one 3-meter High Gain Antenna (HGA), one Medium Gain Antenna (MGA), and two Low Gain Antennas (LGAs) for communications. The HGA would receive signals from the NASA Deep Space Network (DSN) 30-meter antenna on orbit and also downlink science data at orbit. The MGA would only be used for communications with Earth during cruise and when the orbit of the spacecraft around Uranus and the orbit of the Earth make the Earth and spacecraft link close enough for communication. It could also be used to listen for signals from Earth if the spacecraft enters safe mode. The LGAs would only be used for communications during Earth flyby or for communications at distances less than 0.5 AU. When QUEST is in Uranus orbit, the HGA would be the only reliable link to Earth. QUEST would use a Solid-State Power Amplifier (SSPA) and a Small Deep Space Transponder (SDST) with a fully redundant design; both have been flight proven by the Mars Science Laboratory (MSL) [95].

The communications system would use an X-band (7.1 GHz) uplink, and Ka-band downlink (32 GHz) or X-band downlink (7.4 GHz). Note that X-band downlink has a lower data rate, but lower mass and cost. On the

other hand, Ka-band downlink has about 4 times higher data rate versus X-band, but higher mass and cost. X-band downlink is mainly used for cruise phase and Ka-band downlink for science phase. In addition to communication and data transmission, the communications system would also directly contribute to QUEST science investigations. Specifically, X-band downlink would be used for radio occultations to complement the microwave radiometer measurements. Radio science would only be performed during periapsis, and would therefore minimally affect the science downlink capabilities of QUEST. At the end of the mission, both X-band and Ka-band (downlink) would be utilized for gravity science, which therefore requires more power (46 W during transmission of one band at a time versus 69 W during transmission of two bands).

4.4 Science Operations

The QUEST mission science operations would be coordinated based on the spacecraft's proximity to Uranus (Figure 9). Science operations would begin with WAND imaging of Uranus at successively higher resolutions during approach and continue during the insertion orbit and successive 30-day orbits. Within 2 R_U for all orbits, all the instruments would be active and collecting data at the maximum sampling rate and with maximum dynamic range. MIRROR observations would cease at distances greater than 2 R_U, and PRESTO operations would continue until a distance of 12 R_U. In retrospect, we realize that PRESTO operations would benefit from continuing to >=18 R_U in order to help identify magnetic reconnection by measuring the reconnection-associated Whistler waves). The plausibility of this additional operation would need to be studied further. Further from periapse, MAGIC and WAND would continue to collect data at a lower sampling rate, and the periapse data collected would be transmitted to Earth. The nine nominal science orbits are divided into five MIRROR orbits and four RadiAnt orbits; this is due to the pointing requirements of each instrument. During the MIRROR orbits, QUEST would maneuver to maintain nadir pointing of the MIRROR antennas at periapse. For the RadiAnt orbits, the priority would be maintaining line-of-sight between the HGA and Earth for as long as possible. MIRROR would still be collecting data during these RadiAnt orbits, but the off-nadir pointing reduces the precision of brightness temperature measurements. The pointing requirements for the other instruments are not as stringent. The longitudinal coverage of dedicated MIRROR and RadiAnt orbits would provide sufficient data and longitudinal coverage to accomplish the mission objectives.

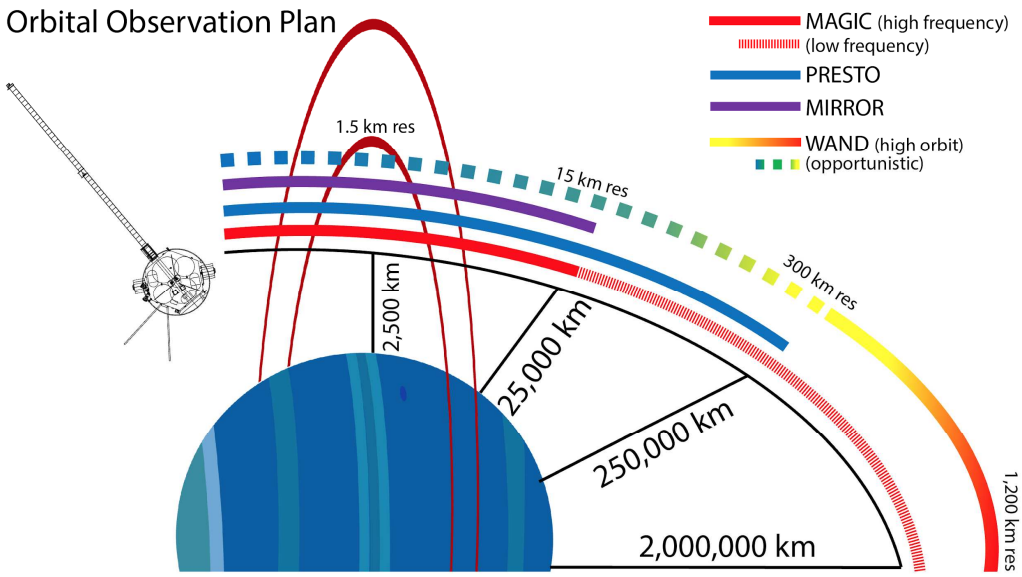

Figure 9. QUEST science operations timeline during insertion and nominal orbits.

5. Programmatics

In the following subsections we describe the notional schedule of our mission design, the Team X validated cost associated with our mission design as well as the perceived mission risks and risk mitigation strategy. All of the following cost information is of a budgetary and planning nature and is intended for informational purposes only.

5.1 Notional Schedule

QUEST's notional schedule is based on previous deep space missions (Juno and New Horizons). Phase A (Concept and Technology Development) and B (Preliminary Design and Technology Completion) are 12 months each, Phase C (Final Design and Fabrication) is 22 months, and Phase D (System Assembly, Integration and Test, and Launch) is 17 months. This timeline is within the median for a Class A mission, as defined by the NASA Procedural Requirements for Risk Classification. Phase E (Operations and Sustainment, not included in the New Frontiers mission cost cap) is 167 months (155 months cruise and 12 months of science).

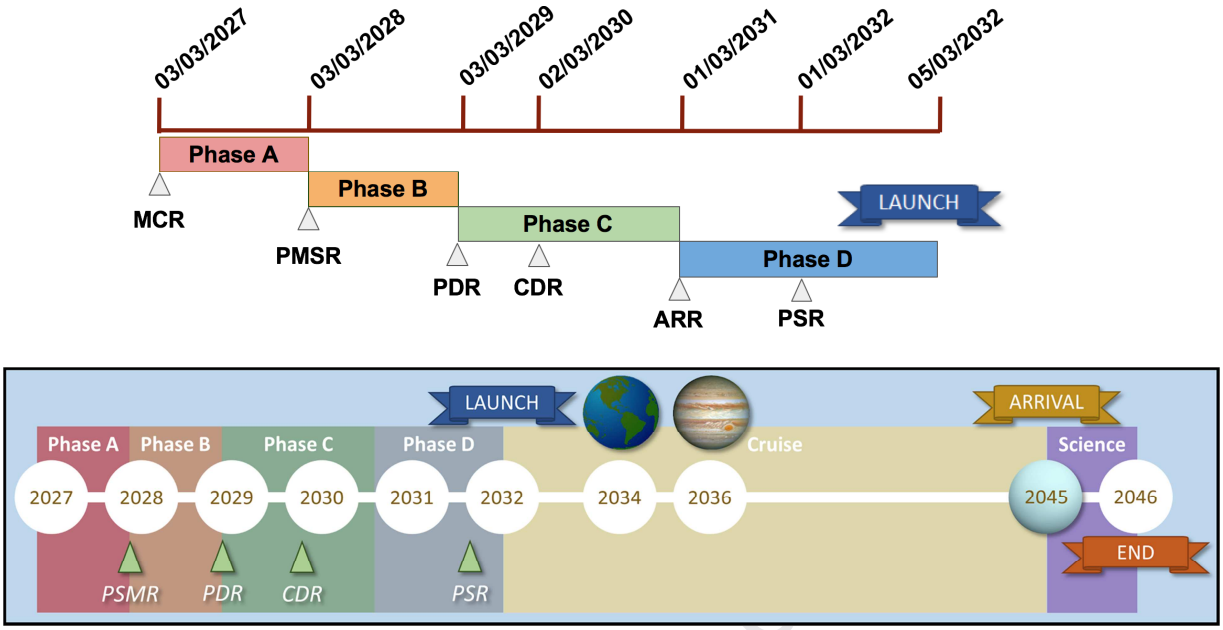

Figure 10. Notional QUEST mission schedule.

The five-year formulation and implementation schedule of the QUEST mission concept shown in Figure 10 includes one month per year of margin for Phases A and B and two months per year of margin for Phases C and D. The key milestones of the mission concept include the Mission Concept Review (MCR) at the beginning of Phase A, the Preliminary Mission and Systems Review (PSMR) at the beginning of Phase B, the Project Design Review (PDR) at the beginning of Phase C, the Critical Design Review (CDR) 11 months after PDR, the Assembly, Test and Launch Operations Readiness Review (ARR) at the beginning of Phase D, the Pre-Ship Review (PSR) one year after ARR, and a launch date of May 3rd 2032, four months after PSR. After launch, the QUEST spacecraft would perform an Earth gravity assist maneuver in 2034, a Jupiter gravity assist while performing a dress rehearsal of UOI, and would arrive at Uranus in 2045 where it would carry out its baseline one-year science mission.

5.2 Projected Cost

We designed QUEST to comply with a cost cap of $900 M FY18 (New Frontiers 4 AO cost cap inflated to FY18 dollars) excluding Phase E and launch vehicle costs. Our total proposed mission cost of $857 M was rigorously validated through a Team X cost model that included real time input from design and technical teams. This is well within the $900M cost cap and also includes 30% reserves (AO requires 25%). The budget includes costs for a non-standard launch vehicle, eMMRTGs (assumed to be the same as MMRTG) and RHUs ($99.7 M). Operations costs (Phases E-F) are estimated to be $227.2M, which is not counted against cost cap and includes 15%

reserves. Table 6 shows the total projected cost summary for our mission concept and Table 7 shows the Phase A-D cost breakdown. The proposed instrument costs shown in Table 8 were determined through the NASA instruments cost model primarily based on Juno instrument costs and the spacecraft costs are provided in Table 9.

Table 6. Projected QUEST cost summary breakdown calculated from the Team X cost model.

Cost Summary	**Team X Estimate**
Phase A-D + Launch Ride + Nuclear Accommodation Costs (NEPA*)	856.7 M
Launch Ride + NEPA costs	99.7 M
Development Cost	757.0 M
Phase A	4.2 M
Phase B	75.7 M
Phase C/D	677.1 M
Phases E-F	227.2 M

*National Environmental Policy Act

Table 7. Projected QUEST Phase A-D development costs.

Total Development Cost (Phase A-D)	**856.7 M**
Project Management	30.9
Project Systems Engineering	29.7
Mission Assurance	23.8
Science	17.6
Payload System	54.9
Flight System	346.0
Mission Operations Prep	19.4
Launch Vehicle	99.7
Ground Data Systems	16.0
ATLO	30.3
Mission and Navigation Design	13.9
Development Reserves	174.6

Table 8. Projected QUEST instrument costs*.

Instruments	**47.7 M**
RadiAnt (Radio Science, part of telecom)	0 M
MAGIC (Magnetometer)	3.8 M
WAND (Wide-angle Camera)	8.3 M
PRESTO (Plasma Wave Receiver)	11.1 M
MIRROR (Microwave Radiometer)	24.4 M

*primarily based on Juno instrument costs

Spacecraft	**306.4 M**
Power	93.2 M
C&DH	28.9 M
Telecom	41.9 M
Structures	41.8 M
Thermal	8.8 M
Propulsion	37.0 M
ACS	19.9 M
Harness	13.5 M
Software	20.0 M
Materials and Processes	1.4 M
Mission and Navigation Design	13.9 M
Development Reserves	174.6 M

Table 9. Projected QUEST spacecraft costs.

5.3 Perceived Risk and Mitigation Strategy

Though there will always be inherent risks with sending a spacecraft billions of kilometers away from the Earth, we assert that our simple, high-heritage spacecraft and instrument suite design would sufficiently mitigate these associated risks. The proposed QUEST mission design was optimized to enable considerable scientific return from 2.6 billion kilometers from Earth under a New Frontiers cost cap. To accomplish this, a long cruise phase (13 years) was chosen due to limitations on available power for propulsion. The 13-year cruise imposes several risks, both technical and programmatic, that must be accounted for. First, the baseline spacecraft power system, two enhanced multi-mission radioisotope thermoelectric generators (eMMRTGs), are nominally rated for a 17-year EODL [92], which could cause early failure or unexpected degradation that would impact the science portion of our mission (year 13-14). Our proposed mitigation strategy involves the inclusion of two eMMRTGs, such that a catastrophic failure of a single unit would not cause mission failure, as well as a healthy 30% power margin (eMMRTGs + Li-ion battery) for the highest-power mode of the spacecraft at end-of-mission (EOM).

With respect to the programmatic risk, a long-duration mission would inevitably involve turnover of mission personnel and the potential for failed transfer of institutional knowledge pertaining to mission operations. To mitigate this, during the long cruise phase there would be monthly meetings of the critical operations team and potential personnel changes would be flagged early to allow for adequate training of new team members and knowledge transfer. The 15% margin in the operations budget could be used to carry out these mitigation strategies, which include regular training, fresh crew cycling, and proficiency tests. Gradual ramp-ups in staffing are anticipated before the critical events, which are Earth Gravity Assist, Jupiter Gravity Assist, and Uranus Orbit Insertion. As was done for the New Horizons mission, the Jupiter Gravity Assist is planned to be used as a full-dress rehearsal (including operational exercises of instruments and ground systems) for Uranus Orbit Insertion which would occur nine years later, providing ample time to address issues that are unanticipated.

A crucial trade that was made during the mission design period was the inclusion of the latest generation of JPL flight avionics (Sphinx processor [93]) for command and data handling, which allowed for continuous power savings of 33 W. The processor has been flight-qualified and delivered for three Class B missions (NEA Scout, Lunar Flashlight, and Peregrine), and would have 10 years of in-flight operations on these missions prior to QUEST PDR (03/2029). As QUEST is a Class A mission, we anticipate the potential for requalification of the Sphinx processor. We have allocated $1 million for Class A ground-based testing prior to PDR to ensure flight-readiness of this technology.

Finally, as our proposed Uranus orbital insertion and subsequent science orbits involve passing within the radius of the Uranus ring system, we identified the ring-plane crossings as a potential risk to the spacecraft. To find a safe location for ring-plane crossing, details of the Uranian ring system were studied, and we decided on a ring-plane crossing through the ζ_{CC} ring, which extends from 27,000 km to 35,000 km in altitude and likely comprises sparse dust with an average diameter of 1 µm [96]. This ring is also constantly being depopulated via atmospheric drag such that the particles have a 100-year lifetime [97]. We compared the anticipated ring plane crossings at Uranus and compared these to the Cassini Grand Finale and determined the risk to QUEST was significantly less than during Cassini's ring-crossings given that QUEST would be travelling at ½ the velocity of Cassini (meaning the kinetic energy of impact will be ¼ for similar size particle), the particle size for the QUEST ring crossing is 1/20th that of the Cassini ring crossings, and QUEST would perform only half the ring crossings of Cassini's Grand

Finale. However, we would advocate for investment in new Earth-based research to better characterize the ring-crossing hazard and further constrain ideal periapse altitude orbit insertion options.

6. Conclusion

In this paper we described a New Frontiers Uranus orbiter mission concept study carried out during the 2018 JPL Planetary Science Summer Seminar. Our proposed mission, QUEST, is a high-heritage mission architecture that aims to remedy the decades-long absence of ice giant missions. The mission is designed to achieve two major goals: to use Uranus as a laboratory to better understand the dynamos that drive magnetospheres in the solar system and beyond, and to determine the relationship between the magnetic environment, thermal environment, winds and deeper thermal-compositional structure of Uranus' interior in contrast with the other giant planets. These goals would directly address the highest priority objectives outlined for a Uranus orbiter flagship class mission in the most recent NASA Decadal Survey within a New Frontiers mission cost cap. The remote and in-situ sensing opportunities only possible with a dedicated mission would provide chemical, thermal, and magnetic markers that are coupled to the formation and migration history of Uranus. These measurements would also yield invaluable ground truth for comparisons to ice giant-size exoplanets, considered the most abundant in our galaxy. In addition, the idiosyncrasies of Uranus (e.g. its anomalously low thermal emission, its oddly-shaped, chaotic magnetic field, and its extreme axial tilt) provide a target that could lead to significant updates to long-standing theories of planetary formation and the effects of planetary extrema.

The proposed QUEST mission concept demonstrates that compelling science objectives can still be met under the significant cost and mass limitations inherent to a New Frontiers-class ice giant mission. Our notional mission architecture consists of a Juno-style spin-stabilized orbiter with a magnetometer, plasma wave receiver, microwave radiometer, wide angle camera, and radio antenna instrument suite capable of investigating Uranus' magnetosphere, atmosphere and interior while also providing opportunities to reveal some information pertaining to the system as a whole. We believe the instruments and mission design approach described here are feasible within the boundaries set by the New Frontiers program, but QUEST is by no means the only possible architecture that could address high priority ice giant mission science goals. We direct the reader to the Ice Giants Pre-Decadal Study [8] for an extensive discussion of dozens of Flagship mission architectures (*e.g.*, flybys, orbiters, and probes) and

their relative scientific merits, and we suggest that the full solution space of New Frontiers options be explored in the future as well.

The QUEST mission cost is estimated at $857 million USD (FY18; excluding launch cost and Phase E-F costs) with 30% margin as well as an orbiter dry mass of 1210 kg. These values put the mission architecture under the New Frontiers cost cap and well within the required mass margins for an Atlas V 551 launch vehicle. Further options for mass-saving exist, including the use of a 4-meter fairing for launch. This mass margin enables mission augmentation, including the possibility of orbital precession using additional propellant, the addition of new instruments, enhancements to currently specified instruments, or the inclusion of an atmospheric probe.

There is significant community support for a Uranus mission as demonstrated by the inclusion of a Uranus orbiter as a high priority mission in the most recent NASA Decadal Survey. As a direct result of this community support, several potential flagship ice giant mission architectures have been investigated [7, 8, 9, 10, 98]. However, funding for a new flagship class mission in the near future is not guaranteed, and the ideal launch window of 2029-2034 for a mission to Uranus is quickly approaching. As the QUEST mission concept shows, it is possible to design compelling Uranus mission concepts within a reduced budget and mass framework, and further development of such concepts is necessary if we wish to visit either of the ice giant planets within the near future.

Acknowledgements

The authors would like to thank the Planetary Science Summer Seminar organizers Joyce Armijo, Leslie Lowes, Karl Mitchell and Charles Budney for their incredible support and mentorship. We would also like to thank William Smythe, Mark Hofstader, Shannon Brown, and Thaddaeus Voss for their guidance, and the members of Team X at JPL for their assistance in developing this mission concept. In addition, we would like to thank Liang Wang at Princeton University for visualizing the 3-D Uranus magnetosphere simulation result from the Gkeyll ten-moment multifluid code that is publicly available at https://bitbucket.org/ammarhakim/gkeyll. This research was carried out at the Jet Propulsion Laboratory, California Institute of Technology, under contract with the National Aeronautics and Space Administration. The information presented about the QUEST mission concept is pre-decisional and is provided for planning and discussion purposes only. The cost information contained in this document is of a budgetary and planning nature and is intended for informational purposes only. It does not constitute a commitment on the part of JPL and/or Caltech.

Acronyms

ACS - Attitude Control System
AO - Announcement of Opportunity
ARR - Assembly, Test and Launch Operations Readiness Review
ATLO - Assembly, Test, and Launch Operations
AU - Astronomical Unit
C3 - "characteristic energy" and is equal to the earth departure V∞2
CAS - Cruise Approach Science
CBE - Current Best Estimate
C&DH - Command and Data Handling
CDR - Critical Design Review
CPU - Central Processing Unit
DSM - Deep Space Maneuver
DSN - Deep Space Network
E0EJU - Earth, Earth, Jupiter, Uranus Trajectory
eMMRTG - enhanced Multi-Mission Radioisotope Thermoelectric Generator
EODL - End of Design Life
EOM - End of Mission
ESA - European Space Agency
Δf/f - change in frequency over frequency?
FPGA - Field-Programmable Gate Array
FOV - Field of View
FWHM - Full Width Half Maximum
FY - Fiscal Year
H2O - Chemical formula for water
H2S - Chemical formula for Hydrogen Sulfide
HGA - High Gain Antenna
Hz - Hertz
IFOV - Instantaneous Field of View
IMU - Inertial Measurement Unit
JPL - Jet Propulsion Laboratory
KBO - Kuiper Belt Object
L/V - Launch Vehicle
LGA - Low Gain Antenna
MAGIC - MAGnetometer investigations of an ICe giant, Magnetometer instrument on QUEST
MCR - Mission Concept Review
MEV - Maximum Expected Value
MGA - Medium Gain Antenna
MIRROR - MIcRowave RadiOmeteR instrument on QUEST
MLI - Multi-Layer Insulation
MPV - Maximum Possible Value
MSL - Mars Science Laboratory
MWR - Microwave Radiometer
NAND - Not-and (A type of transistor arrangement used to create memory)
NASA - National Aeronautics and Space Administration
NEPA - National Environmental Policy Act
NF - New Frontiers
NH3 - Chemical formula for Ammonia
nT - nanotesla
OPAG - Outer Planets Assessment Group
PDR - Preliminary Design Review
ppm - parts per million
PRESTO - Plasma-wave Receiver Exposing Structure of The dynamO, Plasma Wave Receiver on QUEST
PRM - Period Reduction Maneuver
PSMR - Preliminary Mission and System Review

PSR - Pre-Ship Review
PSSS - Planetary Science Summer Seminar
PWR - Plasma Wave Receiver
QUEST - Quest to Uranus to Explore Solar System Theories
RadiAnt - Radio Antenna on QUEST
R_U - Uranus Radii
RHU - Radioisotope Heater Units
RPS - Radioisotope Power System
S/C - Spacecraft
SBAG - Small Bodies Assessment Group
SDST - Small Deep Space Transponder
SEP - Solar Electric Propulsion
SSPA - Solid-State Power Amplifier
TDI - Time Delayed Integration
TEC - Thermoelectric Coupler
TRL - Technology Readiness Level
USD - United States Dollars
UOI - Uranus Orbit Insertion
deltaV - velocity increment or decrement (usually in reference to a spacecraft)
$V\infty$ - speed of the trajectory with respect to a target (departure, flyby or arrival body).
VRHU - variable radioisotope heater units
W - Watts
WAC - Wide Angle Camera
WAND - Wide-Angle methaNe Detector, Camera on QUEST

References

[1] C.S. Arridge, et al., 2014. The Science Case for an Orbital Mission to Uranus: Exploring the Origins and Evolution of Ice Giant Planets. Planetary and Space Science. 104 (Part A), 122–40. doi:10.1016/j.pss.2014.08.009.

[2] A. Masters, et al., 2014. Neptune and Triton: Essential pieces of the Solar System puzzle. Planet. Space Sci. 104 (Part A), 108-121. doi:10.1016/j.pss.2014.05.008.

[3] O. Mousis, et al., 2018. Scientific rationale for Uranus and Neptune in situ explorations, Planet. Space Sci. 155, 12–40.

[4] B. J. Fulton, et al., 2017. The California-Kepler Survey. III. A Gap in the Radius Distribution of Small Planets. The Astronomical Journal. 154, 3. doi:10.3847/1538-3881/aa80eb.

[5] National Aeronautics, Space Administration, 2016. Announcement of Opportunity, New Frontiers 4. NNH16ZDA011O, Washington, DC.

[6] National Research Council, 2011.Visions and Voyages for Planetary Science in the Decade 2013–2022, ISBN 13: 978 0 309 20954 0.

[7] European Space Agency CDF Study Report, 2019. A Mission to the Ice Giants - Uranus and Neptune, ESA CDF-187 (C).

[8] M. Hofstadter, et al., 2017. A Vision for Ice Giant Exploration. LPI Contrib. No. 1989, Planetary Science Vision 2050 Workshop 2017. https://www.lpi.usra.edu/icegiants/mission_study/Full-Report.pdf

[9] S. J. Saikia, et al., 2014. A New Frontiers Mission Concept for the Exploration of Uranus, Abstract #2406 Presented at 2014 LPSC meeting.

[10] C. M. Elder, et al., 2018. OCEANUS: a high science return Uranus orbiter with a low-cost instrument suite. Acta Astronaut. 148, 1–11.

[11] Outer Planets Assessment Group Fall 2018 Findings. https://www.lpi.usra.edu/opag/meetings/sep2018/findings.pdf, Accessed 09/11/2019.

[12] Small Bodies Assessment Group June 2018 Findings. **https://www.lpi.usra.edu/sbag/meetings/jun2018/findings.pdf**, Accessed 09/11/2019.

[13] E. C. Stone, E. D. Miner, 1989. The Voyager 2 encounter with the Uranian system. Science. 233, 39-43.

[14] N. F. Ness, et al., 1986. Magnetic Fields at Uranus. Science. 233, no. 4759, 85–89.

[15] J. C. Pearl, B. J. Conrath, R. A. Hanel, J. A. Pirraglia, A. Coustenis, 1990. The albedo, effective temperature, and energy balance of Uranus, as determined from Voyager IRIS data. Icarus. 84, 12–28.

[16] N. Nettelmann, et al., 2016. Uranus evolution models with simple thermal boundary layers. Icarus. 275, 107–116. https://doi.org/10.1016/j.icarus.2016.04.008.

[17] W. B. Hubbard, J. J. MacFarlane, 2008. Structure and evolution of Uranus and Neptune. J. Geophys. Res. Solid Earth. 85, 225–234. https://doi:10.1029/jb085ib01p00225.

[18] J. Kavelaars O. Mousis, J. M. Petit, H. A. Weaver, 2011. On the formation location of Uranus and Neptune as constrained by dynamical and chemical models of comets. The Astrophysical Journal Letters. 734, 2. doi:10.1088/2041-8205/734/2/L30.

[19] R. Frelikh, R. A. Murray-Clay, 2017. The Formation of Uranus and Neptune: Fine Tuning in Core Accretion. The Astronomical Journal. 154, 3. https://doi.org/10.3847/1538-3881/aa81c7.

[20] R. Helled, P. Bodenheimer, 2014. The Formation of Uranus & Neptune: Challenges and Implications For Intermediate-Mass Exoplanets. The Astrophysical Journal. 789, 1. https://doi.org/10.1088/0004-637X/789/1/69.

[21] K. H. Baines, et al., 2018. Saturn in the 21st Century. Cambridge University Press. 20.

[22] S. K. Atreya, et al., 2019. Icy giant planet exploration: Are entry probes essential? Acta Astronaut. 162, 266-274.

[23] I. de Pater, et al., 2014. Record-breaking storm activity on Uranus. Icarus. 252, 121–128. https://doi.org/10.1016/j.icarus.2014.12.037.

[24] P. G. J. Irwin, M. H. Wong, A. A. Simon, G. S. Orton, D. Toledo, 2017. HST/WFC3 observations of Uranus' 2014 storm clouds and comparison with VLT/SINFONI and IRTF/Spex observations. Icarus. 288, 99–119. https://doi.org/10.1016/j.icarus.2017.01.031.

[25] L. A. Sromovsky, E. Karkoschka, P. M. Fry, H. B. Hammel, I. de Pater, K. Rages, 2014. Methane depletion in both polar regions of Uranus inferred from HST/STIS and Keck/NIRC2 observations. Icarus. 238, 137–155. https://doi.org/10.1016/j.icarus.2014.05.016.

[26] S. J. Bolton, et al., 2017. Jupiter's Interior and Deep Atmosphere: The Initial Pole-to-Pole Passes with the Juno Spacecraft. Science. 6340: 821. https://doi:10.1126/science.aal2108.

[27] K. M. Soderlund, M. H. Heimpel, E. M. King, J. M. Aurnou, 2013. Turbulent models of ice giant internal dynamics: Dynamos, heat transfer, and zonal flows. Icarus. 224, 97–113. https://doi.org/10.1016/j.icarus.2013.02.014.

[28] J. Leconte, F. Selsis, F. Hersant, T. Guillot, 2017. Condensation-inhibited convection in hydrogen-rich atmospheres. Astron. Astrophys. 598, A98. https://doi.org/10.1051/0004-6361/201629140

[29] M. Podolak, W. B. Hubbard, D. J. Stevenson, 1991. Models of Uranus' Interior and Magnetic Field, Uranus, The University of Arizona Press.

[30] J. A. Kegerreis, J.A., 2018. Consequences of Giant Impacts on Early Uranus for Rotation, Internal Structure, Debris, and Atmospheric Erosion. Astrophys. J. 861, 52. https://doi.org/10.3847/1538-4357/aac725

[31] M. S. Marley, C. P. McKay, 1999. "Thermal Structure of Uranus' Atmosphere," Icarus. 138, 2, 268–286.

[32] J. E. P. Connerney, 2015. Planetary magnetism. Volume 10: Planets and Satellites. In G. Schubert and T. Spohn, (Eds.) Treatise in Geophysics, Elsevier, Oxford, UK, 10.06, 195- 237. ISBN: 978-0-444-63803-1.

[33] K. Moore, et. al., 2018. A complex dynamo inferred from the hemispheric dichotomy of Jupiter's magnetic field. Nature. 561, 76-78, doi:10.1038/s41586-018-0468-5.

[34] M. K. Dougherty, et al., 2018. Saturn's magnetic field revealed by the Cassini Grand Finale. Science. 362, 6410, 46. doi:10.1126/science.aat5434.

[35] J. E. P. Connerney, et al., 2018. A New Model of Jupiter's Magnetic Field From Juno's First Nine Orbits. Geophysical Research Letters. 45, 6, 2590–2596. https://doi-org.ezproxy.net.ucf.edu/10.1002/2018GL077312

[36] V. M. Vasyliunas, 1986. The convection-dominated magnetosphere of Uranus. Geophys. Res. Lett. 13, 621–623. https://doi.org/10.1029/GL013i007p00621.

[37] G. Ye, T. W. Hill, 1994. Solar-wind-driven convection in the Uranian magnetosphere. J. Geophys. Res. 99, 17225. https://doi.org/10.1029/94JA00870.

[38] X. Cao, C. Paty, 2017. Diurnal and seasonal variability of Uranus's magnetosphere. J. Geophys. Res. Sp. Phys. 122, 6318–6331. https://doi.org/10.1002/2017JA024063.

[39] C. F. Dong, et al., 2017. The dehydration of water worlds via atmospheric losses. Astrophysical Journal Letters. 847, L4.

[40] C. F. Dong, Z. G. Huang, M. Lingam, 2019a. Role of Planetary Obliquity in Regulating Atmospheric Escape: G-dwarf versus M-dwarf Earth-like Exoplanets, Astrophysical Journal Letters. 882, L16.

[41] L. Wang, et al., 2018. Electron Physics in 3D Two-Fluid Ten-Moment Modeling of Ganymede's Magnetosphere. J. Geophys. Res. Space Physics. 123, 2815-2830.

[42] L. Wang, A. Hakim, J. Ng, C. F. Dong, K. Germaschewski, 2019. Exact and Locally Implicit Source Term Solvers for Multifluid-Maxwell Systems, arXiv:1909.04125.

[43] C. F. Dong, L. Wang, A. Hakim, A. Bhattacharjee, J. A. Slavin, G. A. DiBraccio, K. Germaschewski, 2019. Global Ten0Moment Multifluid Simulations of the Solar Wind Interaction with Mercury: From the Planetary Conducting Core to the Dynamic Magnetosphere. Geophys. Res. Lett., 461, 11584-11596. doi:10.1029/2019GL083180.

[44] G. S. Orton, et al., 2015. Thermal imaging of Uranus: Upper-tropospheric temperatures one season after Voyager. Icarus. 260, 94-102.

[45] N. Nettelmann, R. Helled, J. J. Fortney, R. Redmer, 2013. New indication for a dichotomy in the interior structure of Uranus and Neptune from the application of modified shape and rotation data, Planet. Space Sci. 77, 143–151.

[46] A. C. Mitchell, W. J. Nellis, 1982. Equation of state and electrical conductivity of water and ammonia shocked to the 100 GPa (1 Mbar) pressure range. J. Chem. Phys. 76, 6273–6281. https://doi.org/10.1063/1.443030.

[47] Cavazzoni, et al., 1999. Superionic and metallic states of water and ammonia at giant planet conditions. Science. 283, 44–46. https://doi.org/10.1126/science.283.5398.44

[48] Millot, et al. Nanosecond X-ray diffraction of shock-compressed superionic water ice, 2019. Nature. 569, 251–255. https://doi.org/10.1038/s41586-019-1114-6

[49] G. H. Voigt, K. W. Behannon, N. F. Ness, 1987. Magnetic field and current structures in the magnetosphere of Uranus. J. Geophys. Res. 92, 15337–15346. https://doi.org/10.1029/JA092iA13p15337

[50] Y. Kaspi, et al., 2013. Atmospheric confinement of jet streams on Uranus and Neptune. Nature. 497, 7449, 344–347. https://doi-org.ezproxy.net.ucf.edu/10.1038/nature1213.

[51] R. Helled, J. D. Anderson, M. Podolak, G. Schubert, 2011. "Interior Models of Uranus and Neptune," Astrophys. J. 15.

[52] J. E. P. Connerney, M. H. Acuña, N. F. Ness, 1987. The magnetic field of Uranus, Journal of Geophysical Research - Space Physics. 92, 15329-15336.

[53] R. Holme, and J. Bloxham, 1996. The magnetic fields of Uranus and Neptune: Methods and models, Journal of Geophysical Research, 101, 2177-2200.

[54] S. Stanley, J. Bloxham, 2006. Numerical dynamo models of Uranus' and Neptune's magnetic fields. Icarus. 184, 556–572.

[55] S. Gulkis, M. A. Janssen, E. T. Olsen, 1978. Evidence for the depletion of ammonia in the Uranus atmosphere, Icarus. 34, 10-19.

[56] I. de Pater, P. N. Romani, S. K. Atreya, 1991. Possible microwave absorption by H2S gas in Uranus' and Neptune's atmospheres. Icarus. 91, 220-233

[57] S. K. Atreya, K. H. Baines, P. A. Egeler, 2006. An Ocean Of Water-ammonia On Neptune And Uranus: Clues From Tropospheric Cloud Structure. American Astronomical Society, DPS meeting No.38, id.05.08; Bulletin of the American Astronomical Society, 38, 489.

[58] J. Birn and E. R. Priest, 2007. Reconnection of Magnetic Fields: Magnetohydrodynamics and Collisionless Theory and Observations. Cambridge University Press.

[59] M. G. Kivelson and C. T. Russell, 1995. Introduction to Space Physics. Cambridge University Press.

[60] J. A. Slavin, et al., 2009. MESSENGER Observations of Magnetic Reconnection in Mercury's Magnetosphere. Science. 324, 5927, 606-610.

[61] S. A. Fuselier and W.S. Lewis, 2011. Properties of Near-Earth Magnetic Reconnection from In-Situ Observations. W.S. Space Sci Rev, 160:95. https://doi.org/10.1007/s11214-011-9820-x.

[62] R. W. Ebert, et al., 2017. Accelerated flows at Jupiter's magnetopause: Evidence for magnetic reconnection along the dawn flank. Geophysical Research Letters, 44, 10.

[63] R. L. Guo, et al., 2018. Rotationally driven magnetic reconnection in Saturn's dayside. Nature Astronomy. 2, 640-645. doi:10.1038/s41550-018-0461-9.

[64] G. A. DiBraccio and D. J. Gershman. Voyager 2 constraints on plasmoid-based transport at Uranus. Geophysical Research Letters. 46, 19. https://doi.org/10.1029/2019GL083909.

[65] J. W. Dungey, 1961. Interplanetary Magnetic Field and the Auroral Zones. Phys. Rev. Lett. 6, 47.

[66] J. Yoo, et al., 2018. Whistler Wave Generation by Anisotropic Tail Electrons During Asymmetric Magnetic Reconnection in Space and Laboratory. Geophysical Research Letters. 45, 16. https://doi.org/10.1029/2018GL079278.

[67] G. DiBraccio, et al., 2012. MESSENGER observations of magnetopause structure and dynamics at Mercury. JGR Space Physics. 118, 997-1008. doi:10.1002/jgra.50123, 2013.

[68] T. L. Zhang, et al., 2016. Magnetic Reconnection in the Near Venusian Magnetotail. Science. 336, 6081, 567-570. doi: 10.1126/science.1217013.

[69] S. J. Weidenschilling , J. S. Lewis, 1973. Atmospheric and cloud structures of the Jovian planets. Icarus. 20:465–476. doi: 10.1016/0019-1035(73)90019-5.

[70] J. E. P. Connerney, et al., 2017. Juno Magnetic Field Investigation. Space Science Reviews. 1–4: 39. doi:10.1007/s11214-017-0334-z.

[71] M. D. Desch, et al., 1989. Uranus as a Radio Source. In: Uranus, University of Arizona Press.

[72] W. S. Kurth, D. A. Gurnett, F. L. Scarf, F. V. Coroniti, 1989. Wave-Particle Interactions in the Magnetosphere of Uranus. In: Uranus, eds. Bergstralh et al., University of Arizona Press.

[73] J. W. Warwick, et al., 1986. Voyager 2 Radio Observations of Uranus. Science. 233, 4759, 102-106. doi:10.1126/science.233.4759.102

[74] D. A. Gurnett, W. S. Kurth, F. L. Scarf, R. L. Poynter, 1986. First plasma wave observations at Uranus. Science. 4759, 106-109. doi:10.1126/science.233.4759.106.

[75] F. L. Scarf, et al., 1987. Plasma Wave Measurements in the Magnetosphere of Uranus. JGR. 92, A13, 15,217-15,224.

[76] D. A. Gurnett, et al., 2004. The Cassini Radio and Plasma Wave Investigation, Space Science Reviews. 114, 395-463.

[77] I. de Pater, D. DeBoer, M. Marley, R. Freedman, R. Young, 2005. Retrieval of Water in Jupiter's Deep Atmosphere Using Microwave Spectra of Its Brightness Temperature. Icarus. 173, 2, 425–38.

[78] J. Polívka, 1995. Microwave radiometry and applications. Int. J. Infrared Millimeter Waves. 16, 1593–1672. https://doi.org/10.1007/BF02274819.

[79] M. A. Janssen, et al., 2017. MWR: Microwave Radiometer for the Juno Mission to Jupiter. Space Sci. Rev. https://doi.org/10.1007/s11214-017-0349-5.

[80] C. Li, et al., 2017. Microwave observations of Jupiter's atmosphere from 1 bar to 200 bars. American Geophysical Union, Fall Meeting 2018, abstract #P33F-3884.

[81] M. D. Hofstadter, V. Adumitroaie, S. Atreya, B. Butler, 2018. Probing the Atmospheres of Saturn and Uranus with Ground-Based Radio Observations. EPSC Abstracts, 12.

[82] P. G. J. Irwin, et al., 2019. Probable detection of hydrogen sulphide (H2S) in Neptune's atmosphere. Icarus. 321, 550-563. doi: 10.1016/j.icarus.2018.12.014.

[83] Y. Zhang, et al., 2018. A 2.6GS/s Spectrometer System in 65nm CMOS for Spaceborne Telescopic Sensing, 2018 IEEE International Symposium on Circuits and Systems. https://doi.org/10.1109/ISCAS.2018.8351690.

[84] Y. Zhang, et al., 2019. Integrated Wide-Band CMOS Spectrometer Systems for Spaceborne Telescopic Sensing, IEEE Trans. Circuits Syst. 66, 1863-1873. https://doi.org/10.1109/TCSI.2019.2896850.

[85] R. Hughes, et al., 2012. Mechanical development of a very non-standard patch array antenna for extreme environments, 2012 IEEE Aerospace Conference. https://doi.org/10.1109/AERO.2012.6187093.

[86] T. Owen, T. Encrenaz, 2006. Compositional constraints on giant planet formation. Planetary and Space Science. 54, 12, 1188–1196. https://doi-org.ezproxy.net.ucf.edu/10.1016/j.pss.2006.05.030.

[87] V. R. Eshleman, 1973. The radio occultation method for the study of planetary atmospheres. Planet. Space Sci. 21, 1521–1531. https://doi.org/10.1016/0032-0633(73)90059-7.

[88] G. F. Lindal, et al., 1987. The Atmosphere of Uranus: Results of Radio Occultation Measurements with Voyager 2. Journal of Geophysical Research. 92, No A13, 14, 987-15, 001. https://doi.org/10.1029/JA092iA13p14987.

[89] C. J. Hansen, et al., 2017. Junocam: Juno's Outreach Camera. Space Science Reviews. 1–4, 475.

[90] S. K. Croft, L. A. Soderblom, 1991. Geology of the Uranian Satellites, in Uranus (A92018701 05-91). Tucson, AZ, University of Arizona Press, 561-628.

[91] A. P. Ingersoll, et al., 1998. Imaging Jupiter's Aurora at Visible Wavelengths. Icarus. 1: 251.

[92] D. Woerner, 2016. Journal of Electronic Materials 45: 1278. https://doi.org/10.1007/s11664-015-3998-8.

[93] CubeSat Flight System Development for Enabling Deep Space Science, 2017. 2017 IEEE Aerospace Conference, 1. doi:10.1109/AERO.2017.7943885.

[94] Y. Kasahara, Y. Goto, S. Yamawaki, H. Matsui, 2014. Evaluation of Data Compression Techniques Applicable for Plasma Wave Instruments, in: Proc. of European Planetary Science Congress.

[95] T. J. Martin-Mur, G. Kruizinga, M. Wong, 2013. Mars science laboratory interplanetary navigation performance. J. Spacecr. Rockets. 148, 473–485. https://doi.org/10.2514/1.A32631.

[96] D. E. Dunn, I. de Pater, D. Stam, 2010. Modeling the uranian rings at 2.2 μm: Comparison with Keck AO data from July 2004. Icarus. 208, 927–937. https://doi.org/10.1016/j.icarus.2010.03.027.

[97] A. L. Broadfoot, et al., 1986. Ultraviolet spectrometer observations of Uranus. Science. 233, 74–79. https://doi.org/10.1038/ajg.2013.400.

[98] D. Turrini, et al., 2014. The comparative exploration of the ice giant planets with twin spacecraft: Unveiling the history of our Solar System. Planet Space Sci. 194, 93-107. https://doi.org/10.1016/j.pss.2014.09.005.

Vitae

Stephanie Jarmak

Stephanie Jarmak is a doctoral candidate in the University of Central Florida Planetary Science PhD program. She received her B.S. in Earth, Atmospheric and Planetary Sciences (2013) from Massachusetts Institute of Technology and her M.S. in Physics (2015) from Texas A&M University-Commerce. She is currently a graduate research assistant in the Center for Microgravity research where she aids in the development and execution of microgravity experiments designed to study the early stages of planet formation on various platforms including a laboratory drop tower, parabolic and suborbital flights, and CubeSat missions.

Erin Leonard

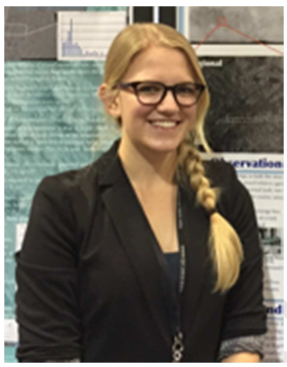

Erin Leonard is a recent PhD graduate in Planetary Geology at the University of California Los Angeles. Her dissertation focuses on geomorphologic mapping of Europa and Enceladus, structural analysis of surface features on these bodies, and physical analogue experiments which replicate conditions on icy satellites. She has immersed herself in the planetary science community at the Jet Propulsion Laboratory throughout her PhD, working closely with Dr. Robert Pappalardo. As a result, she is now one of the only graduate students with the title Europa Clipper Science Affiliate. Erin was also recently Project Manager for the NASA Planetary Science Summer Seminar in which she aided in designing and developing a New Frontiers style mission to Uranus to explore this unique “exoplanet in our backyard”.

Alex Akins

Alex Akins is a current Ph.D. candidate in Electrical and Computer Engineering at Georgia Tech interested in planetary remote sensing and all aspects of satellite mission design. As an undergraduate, his research activity focused primarily on telecommunications and data systems engineering for CubeSat missions. For his graduate research, Alex focuses on microwave and millimeter-wavelength radiometry as a tool to study atmospheric processes. He currently uses results from laboratory measurements and atmospheric radiative transfer modeling to interpret observations of Venus made with millimeter wavelength radio telescope arrays.

Emma Dahl

Emma Dahl is a Ph.D. candidate at New Mexico State University studying planetary science, observational astronomy, and astronomical instrumentation. She is part of the international ground-based observing campaign in support of the *Juno* mission to Jupiter. Using radiative transfer tools, and with context from *Juno* data, she is currently analyzing optical hyperspectral image cubes taken during the spacecraft's close perijove passes to determine the vertical structure of Jupiter's uppermost cloud deck.

Daniel Cremons

Dr. Cremons received his B.A. in Chemistry from Carleton College in Northfield, MN. He went on to obtain a M.S. and Ph.D. in Materials Science from the University of Minnesota. He is currently a Post-doctoral Fellow at NASA Goddard Space Flight Center in Greenbelt, MD working in the Planetary Geology, Geophysics, Geochemistry Laboratory. His research is focused on spectral and Doppler lidar instrument development for atmospheric and surface science on the moon, Mars, Titan, and small bodies.

Shannon Cofield

Shannon Cofield's PhD research focuses on the provenance of iron-oxides in icerafted debris as a proxy for paleo-ice drift patterns in the Arctic Ocean. During an internship at JPL, she applied her geologic knowledge and skills to HiRISE orbital geologic mapping (1:500) and stratigraphic analysis of the clay trough along MSL-Curiosity's extended traverse in Gale crater, Mars. As an external student contributor, her work has been incorporated into the Landing Site Working Groups, as well as the upcoming 4th Landing Site Workshop.

Aaron Curtis

Aaron Curtis received a B.A. in geography from Cambridge University, a M.S. in geochemistry and a Ph.D. in earth science from New Mexico Institute of Mining and Technology in 2016. He participated in seven Antarctic field seasons as lead caver for the Mount Erebus Volcano Observatory, and worked on quadcopters for physical sample collection and sensor placement at Los Alamos National Labs. As a postdoc at NASA JPL, his projects have included IceWorm (the world's first ice climbing robot), Europa Lander, the MoonDiver mission proposal, and fumarole sampling and unmanned aerial vehicle work.

Chuanfei Dong

Chuanfei Dong is an Associate Research Astrophysicist at the Department of Astrophysical Sciences, Princeton University. He received his B. Sci. (2009) from the University of Science and Technology of China in Geophysics and Theoretical Physics. He received his M. Sci. (2010) from Georgia Tech in Earth and Atmospheric Sciences. He received his M. Sci. (2012) and Ph. D. (2015) from the University of Michigan, Ann Arbor in Space and Planetary Sciences, M.S.E. (2014) in Nuclear Engineering and Radiological Sciences, and Ph. D. (2015) in scientific computing. He has received three NASA Group Achievement Awards, EAS Young Researcher Award, and National Academy of Science New Leaders in Space Science.

Emilie Dunham

Emilie Dunham is a PhD candidate and NASA Earth and Space Sciences Fellow at Arizona State University. She studies the oldest meteorite inclusions to better understand Solar System formation at the Center for Meteorite Studies and is advised by Prof. Meenakshi Wadhwa.

Baptiste Journaux

Dr. Baptiste Journaux is a postdoctoral researcher at the Department of Earth and Space Science of the University of Washington. He received his B.S. in Planetary Science from the Sorbonne University, Paris, France, and his Ph.D. in experimental Mineral Physics and Planetary Sciences from École Normale supérieure de Lyon, France. He is currently part of the Titan and Icy Worlds node of the NASA Astrobiology Institute. His research interests use high pressure experiments and advance thermodynamic modeling to identify and characterize the chemical and physical limiting factors for habitability of deep extraterrestrial oceans in icy moons and water-rich exoplanets.

David Murakami

Dr. Murakami is an aerospace engineer in the Experimental Aero-Physics Branch at NASA Ames Research Center, and received his doctorate from the Department of Aeronautics and Astronautics at Stanford University. In his dissertation he developed a mission concept and a novel actively-cooled leading edge to exploit the intense heat generated during planetary entry to propel aerogravity assist vehicles. He has worked on a diverse range of projects including space traffic management, UAV inspection systems, millimeter-wave powered launch vehicles, wind tunnel testing, and thermal protection systems testing; contributing in varied roles including test engineering, instrumentation development, and project management.

Wanyi Ng

Wanyi Ng grew up attending public school in Flagstaff, Arizona. She then attended Duke University for a Bachelor of Science in Mechanical Engineering. She received her Master of Science in Aerospace Engineering from University of Maryland for her research on batteries and fuel cells in electric vertical take-off and landing (eVTOL) rotorcraft. She now works at NASA Goddard Space Flight Center as a propulsion engineer, where she performs analysis, integration, and test of space propulsion systems. Thus far, she has supported the Europa Clipper and WFIRST missions.

Marcus Piquette

Marcus Piquette is a PhD candidate at the University of Colorado at Boulder working with Dr. Mihaly Horanyi on studies of the interplanetary dust distribution. He works on data analysis and instrument calibration for the Student Dust Counter aboard the New Horizons mission to Pluto and the Kuiper Belt. He was born in Gunnison, Colorado and enjoys spending time in the mountains. In his additional spare time he pursues hobbies such as amateur woodworking and playing the drums.

Athul Pradeepkumar Girija

Athul Pradeepkumar Girija is a Ph.D. candidate in School of Aeronautics and Astronautics at Purdue University. He obtained his Bachelors and Masters degrees in Aerospace Engineering from the Indian Institute of Technology, Madras. His Ph.D. dissertation work focuses on the development of a novel systems framework and software tool for aerocapture mission analysis. He is particularly interested in Venus and ice-giant mission concepts and science investigations.

Kimberley Rink

Kimberly Rink is a systems engineer at the Jet Propulsion Laboratory, where she works on planning and sequencing for the Mars Science Laboratory (MSL) Curiosity rover. Kimberly received a BS in Aeronautical and Astronautical Engineering from Purdue University in 2017. She received her master's degree in Aeronautics and Astronautics from Purdue in 2019, where she worked with Dr. Karen Marais to study how novice engineers in the aerospace industry use knowledge management tools to make engineering decisions.

Lauren Schurmeier

Lauren Schurmeier recently received her Ph.D. in Earth and Environmental Sciences from the University of Illinois at Chicago. For her dissertation she investigated the evolution of surface features (craters, mountains, labyrinth terrains) on Saturn's moon Titan using finite element modeling, mapping, and scaling relationships. She received her B.S. in Earth Science concentrating in Planetary Science at the University of California, Santa Cruz. Her research interests include astrobiology, topographic support, ice shell dynamics, and cryovolcanism. She plans to start postdoctoral research at the University of Hawai'i at Mānoa.

Nathan Stein

Nathan Stein is a Ph.D. candidate in Geological and Planetary Sciences at Caltech. He is interested in the remote sensing of planetary surfaces. He is a student collaborator on the ongoing Curiosity mission, where he focuses on characterizing the stratigraphy of the Murray fm. He is also a collaborator on the Dawn mission, where he focuses on the formation and evolution of Na-carbonate deposits on Ceres.

Nicholas Tallarida

Dr. Tallarida is currently working on the development of several prototype *in situ* planetary science instruments as a NASA Postdoctoral Fellow at the Jet Propulsion Laboratory. These instruments range from Raman spectrometers for mineral and organic analysis to a flow cytometer for bacterial life detection and concentration. He received his Ph.D. in Physical Chemistry from the University of California Irvine for his work on high-resolution tip-enhanced Raman spectroscopy.

Myriam Telus

Dr. Telus is an assistant professor in Earth and Planetary Sciences at the University of California Santa Cruz. Dr. Telus is interested in constraining the timing of accretion and evolution of planetesimals via analyses of stable and radiogenic nuclide systems in a wide variety of planetary samples, including primitive meteorite and samples returned from primitive bodies. Specifically, she has made contributions to understanding the 60Fe-60Ni and 26Al-26Mg systematics of chondrules in primitive meteorites (Telus et al., 2012; 2014, 2016, and 2018) and in understanding formation of calcium carbonates in planetesimals (Telus et al., 2019).

Leslie Lowes

Leslie Lowes received a B.S. in Physics from The University of Texas at Arlington in 1981 and a M.S. in Applied Mathematics from California State University-Los Angeles in 1991. She has worked at JPL for the past 12 years, serving as the Galileo Mission to Jupiter Education Lead for 2 years, the Solar System Education Forum Manager until 2009, and the Informal Education Specialist from 2010 until present.

Charles Budney

Dr. Charles J. Budney received a B.S. in Geochemistry from Caltech in 1988 and his Ph.D degree in Geology and Geophysics from the University of Hawaii at Manoa in 1997. He is a senior systems engineer at the Jet Propulsion Laboratory, California Institute of Technology, where he is currently involved in planning for future missions to Mars and working to get NASA data into the decisional processes for water use in tehw estern U.S. He has worked at JPL for over 20 years.

Karl Mitchell

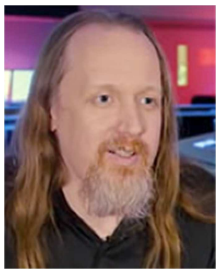

Dr. Karl Mitchell received a B.Sc. in Physics with Space Science and Technology from Leicester University in 1995, an M.Sc. in Remote Sensing from the University of London in 1996, and his Ph.D. in Environmental Science from Lancaster University in 2002. In 2005 he moved to Jet Propulsion Laboratory, California Institute of Technology, initially as a postdoctoral researcher working on the Cassini project, and from 2008 as a staff scientist. His research focuses primarily on geological fluid dynamics, science mission formulation and remote sensing techniques spanning multiple Solar System bodies, especially Titan, Triton and Enceladus. Dr. Mitchell teaches mission formulation, played a number of roles on the Cassini mission, and is Project Scientist for the Discovery 2019 Trident proposal, a mission to Neptune's moon Triton.

Table 1. The QUEST science traceability matrix: high-level science goals, specific science objectives along with the measurement requirements, instrument requirements, and mission architecture requirements to achieve the listed objectives. *Due to the limited scope of our study, investigation into the specific instrument operations required to achieve this objective was not fully explored (see Section 2.2.2) and would require further study for verification.

Science Goal	**Science Objectives**	**Scientific measurement requirement**		**Instrument**	**Instrument functional Requirements**		**Instrument performance**	**Mission requirements**
		Physical parameters	**Observables**		**Function**	**Requirement**		
Understanding dynamos that drive magnetospheres in the solar system and beyond	Distinguish between dynamo models for generation of the magnetic field	Magnetic field vectors and components	Magnetic field direction (20 mrad) and magnitude (0.1% of magnetic field) every 400 meters	Magnetometer	Range	+/- 20,000 nT	+/- 30,000 nT	Multiple orbits with periapsis ≤ 1.1 R_U.
					Resolution	0.1 nT	0.05 nT	
					Sampling rate	50 vectors/sec	100 vectors/sec	
		Electromagnetic perturbation	Radio emissions and plasma waves from open magnetic field regions	Plasma Wave Receiver	Frequency range	10 Hz to 5 MHz	1 Hz to 16 MHz	Multiple orbits with periapsis ≤ 1.1 R_U.
					Frequency resolution	5% ($\Delta f/f$)	1% ($\Delta f/f$)	
					Temporal resolution	4 s (Δt)	4 s (Δt)	
		Location of convective cells as a function of latitude and longitude	Brightness temperature	Microwave Radiometer	Inversion temperature precision	10 K	1 K	Multiple orbits with periapsis ≤ 1.1 R_U. Latitudinal coverage. Take data at multiple emission angles.
					IFOV	27°	20°	
Identifying the energy transport mechanisms in Uranus' magnetic, atmospheric, and interior	Investigate the prediction that Uranus' magnetosphere opens and reconnects daily*	Magnetic field vectors and components as a function of time	Magnetic field direction (0.5°) and magnitude 10 nT	Magnetometer	Range	+/- 20,000 nT	+/- 30,000 nT	Multiple orbits with periapsis ≤ 1.1 R_U and measurements at distances > 18 R_U.
					Resolution	0.1 nT	0.05 nT	
					Sampling rate	50 vectors/sec	100 vectors/sec	

environments in contrast with the other giant planets		Electromagnetic perturbation	Whistler waves associated with magnetic reconnection	Plasma Wave Receiver	Frequency range	1 Hz to 1 kHz	1 Hz to 16 MHz	Multiple orbits at distances > 18 $R_{U.}$
					Frequency Resolution	5% ($\Delta f/f$)	1% ($\Delta f/f$)	
					Temporal Resolution	4 s (Δt)	4 s (Δt)	
	Establish whether surficial winds and banded structure of Uranus' upper atmosphere are related to deeper internal dynamics.	NH_3 and H_2S, gas volume mixing ratios as functions of depth and latitude	Brightness temperature as a function of emission angle (30° range) and latitude	Microwave Radiometer	IFOV	27°	10° to 20°	Need latitudinal and emission angle coverage. S/C spin along line of longitude, polar orbit.
					Integration time	100 ms	100 ms	
					Inversion temperature precision	Model input required	1 K	
		Cloud structure in the upper atmosphere	Visible images of high cloud features and images in 727 nm methane band	Wide-angle Camera	Spatial resolution	1000 km	300 to 600 km	Imaging away from periapsis
					Exposure time	3 ms	3 ms	
	Determine the explanation for Uranus' low thermal emission compared with Neptune and the other giant planets.	Temperature profile of upper atmosphere (0.2 to 2000 mbar)	Ka-band and X-band amplitude and X-band frequency changes	High-gain Antenna	Frequency resolution	0.1 Hz	0.1 Hz	Occultation observation geometry
					Amplitude resolution	1000 ppm	100 ppm	
		Presence of a conductive layer in the atmosphere	Apparent deviation of atmospheric lapse rate (5 K)	Microwave Radiometer	Inversion temperature precision	2 K	1 K	Periapsis, radiometer facing planet every rotation. Spin along line of longitude, polar orbit.
		Distribution, depth, and	Brightness temperature as a	Microwave Radiometer	Radiometer frequency	< 1 GHz	3 GHz to 600 MHz, 8 channels variable	Periapsis, radiometer facing

	relative concentration of NH_3 and H_2S, from 2 bar to ~200 bar	function of emission angle and altitude down to 200 bar		Inversion temperature accuracy	Model input required	0.1 %	planet every rotation. Spin along line of longitude, polar orbit.

Table 2. QUEST instrument suite mass, power, data rate, and heritage information.

Instrument	Mass (kg)	Power (W)[1]	Data per orbit (Mb)[2]	Heritage
MAGIC (magnetometer)	1.5	4	18	MAG (Juno)
PRESTO (plasma wave receiver)	6	6	3780	Waves (Juno), RPWS (Cassini)
MIRROR (microwave radiometer)	42	33	356.4	MWR (Juno)*
RadiAnt (radio antenna)	14.4	80.7[3]	N/A	New Horizons, Cassini
WAND (wide-angle camera)	10.5	7	2400	MVIC (New Horizons), JunoCam (Juno)*

[1]Listed values are average power unless otherwise noted.
[2]Listed values are data per science orbit in megabits, uncompressed
[3]Peak power
*instrument is significantly modified from heritage design

Table 3. ΔV Budget.

Maneuver	ΔV (m/s)
DSM	647.4
DSM Biasing & Flyby Targeting	42.4
UOI	949.6
Period Reduction	83.2
Disposal	15
Total	**1737.6**

Table 4. Per-orbit instrument data volumes.

Instrument	Data volume per orbit (raw, Mb)	Data volume per orbit (loss compression, Mb)
MAGIC	18	18
PRESTO	3780	1890
MIRROR	356.4	356.4
WAND	2400	1200
RadiAnt	N/A	N/A
Total	**6454.4**	**3464.4**

Table 5. Mission total data volumes.

Mission data volume (9 orbits)	Data (Mb)
Instruments, raw	57564
Instruments, compressed	29754
Available Ka-band downlink	36540
Available onboard storage (NAND flash)	64000

Table 6. Projected QUEST cost summary breakdown calculated from the Team X cost model.

Cost Summary	Team X Estimate
Phase A-D + Launch Ride + Nuclear Accommodation Costs (NEPA*)	856.7 M
Launch Ride + NEPA costs	99.7 M
Development Cost	757.0 M
Phase A	4.2 M
Phase B	75.7 M
Phase C/D	677.1 M
Phases E-F	227.2 M

*National Environmental Policy Act

Table 7. Projected QUEST Phase A-D development costs.

Total Development Cost (Phase A-D)	856.7 M
Project Management	30.9
Project Systems Engineering	29.7
Mission Assurance	23.8
Science	17.6
Payload System	54.9
Flight System	346.0
Mission Operations Prep	19.4
Launch Vehicle	99.7
Ground Data Systems	16.0
ATLO	30.3
Mission and Navigation Design	13.9
Development Reserves	174.6

Table 8. Projected QUEST instrument costs*.

Instruments	**47.7 M**
RadiAnt (Radio Science, part of telecom)	0 M
MAGIC (Magnetometer)	3.8 M
WAND (Wide-angle Camera)	8.3 M
PRESTO (Plasma Wave Receiver)	11.1 M
MIRROR (Microwave Radiometer)	24.4 M

*primarily based on Juno instrument costs

Table 9. Projected QUEST spacecraft costs.

Spacecraft	**306.4 M**
Power	93.2 M
C&DH	28.9 M
Telecom	41.9 M
Structures	41.8 M
Thermal	8.8 M
Propulsion	37.0 M
ACS	19.9 M
Harness	13.5 M
Software	20.0 M
Materials and Processes	1.4 M
Mission and Navigation Design	13.9 M
Development Reserves	174.6 M

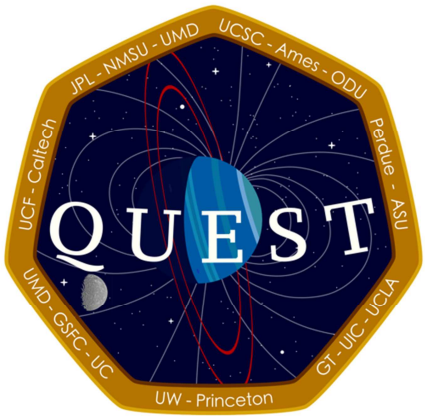

Figure 1. The QUEST mission logo designed by participant Baptiste Journaux depicting the Uranus environment including its obliquity and unique offset magnetic field. The heptagon design represents Uranus as the 7th planet and was inspired by the New Horizons nonagon mission patch.

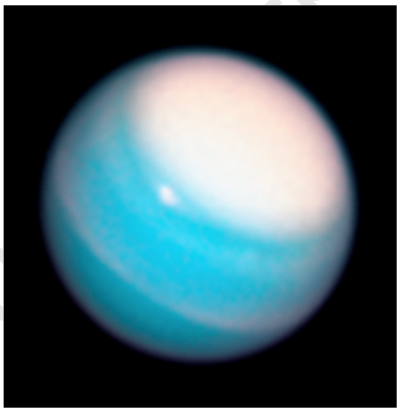

Figure 2. Hubble Space Telescope image taken in September 2018 revealing Uranus' vast polar cap and a bright, persistent storm. Credits: NASA, ESA, A. Simon (NASA Goddard Space Flight Center), and M.H. Wong and A. Hsu (University of California, Berkeley).

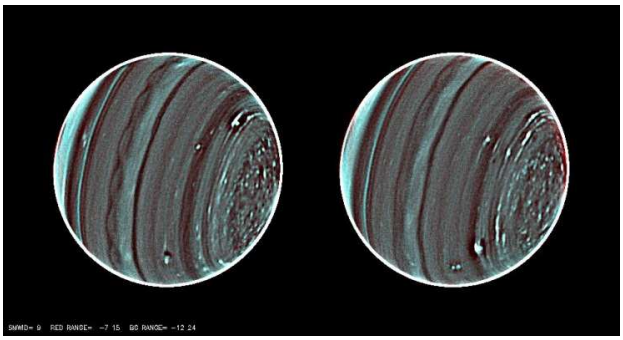

Figure 3. High contrast Keck telescope observations of Uranus in 2012 revealing distinct clouds and banded structures similar to the other giant planets in contrast with the seemingly passive exterior observed during the Voyager 2 flyby in 1986. Credit: NASA / ESA / L. A. Sromovsky / P. M. Fry / H. B. Hammel / I. de Pater / K. A. Rages.

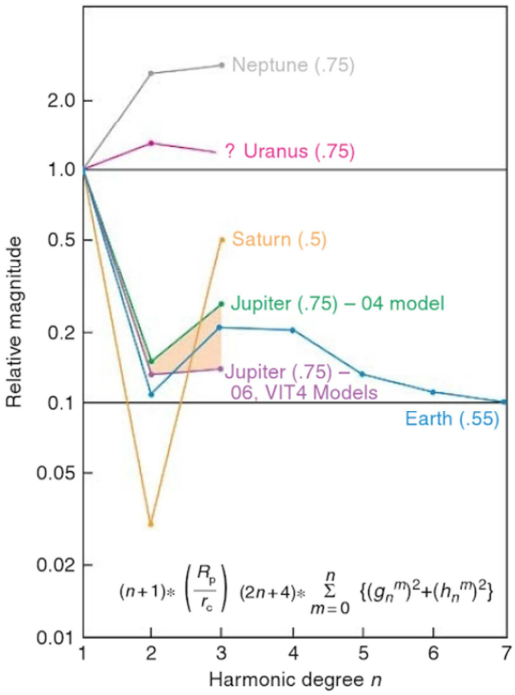

Figure 4. Relative harmonic content of spherical harmonic models of Jupiter, Saturn, Uranus and Neptune compared to Earth, normalized to the assumed core radius for each planet [32].

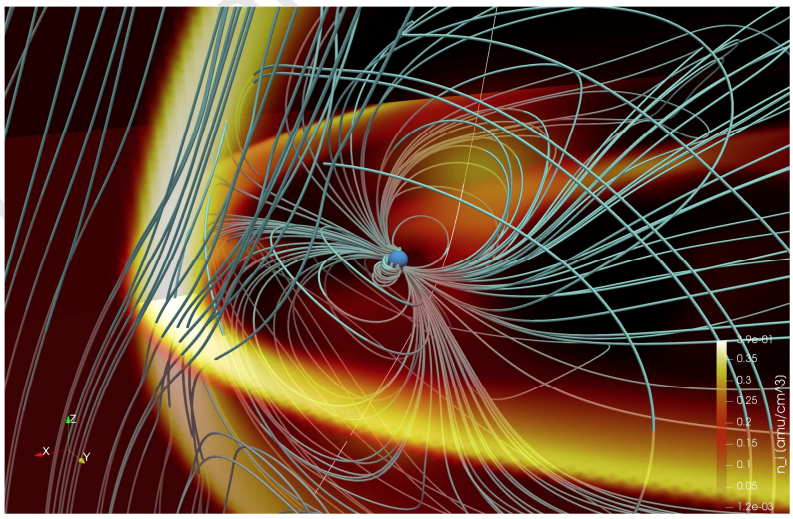

Figure 5. Depiction of Uranus' complex magnetic field interaction with incident solar wind from the ten-moment multifluid magnetosphere simulation (for model details, please refer to [41, 42] and [43]. The color contours depict the proton density in cm^{-3}. The magnetic field lines are presented in cyan. Open and closed field lines on the dayside magnetosphere result from magnetic reconnection between the interplanetary magnetic field and planetary magnetic field.

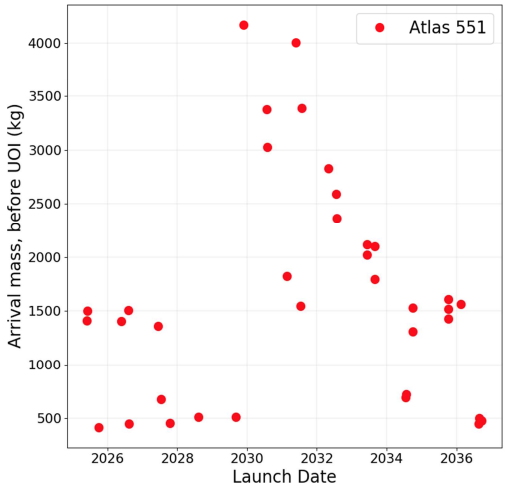

Figure 6. Arrival mass values for launch windows between 2025 and 2037 using the Atlas V551 launch vehicle. A Jupiter gravity assist available between 2030 - 2032 launch dates yield a significant increase in deliverable mass.

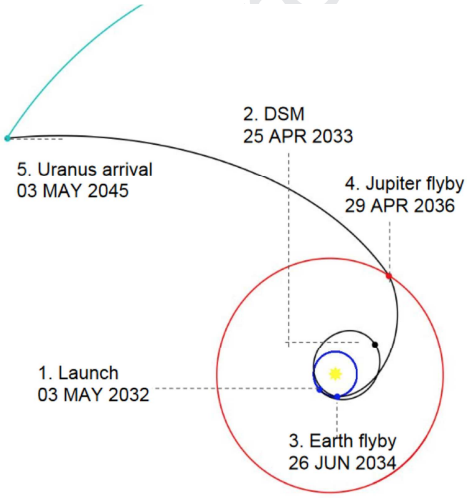

Figure 7. 13-year E0EJU trajectory selected for the mission concept (0 indicates DSM).

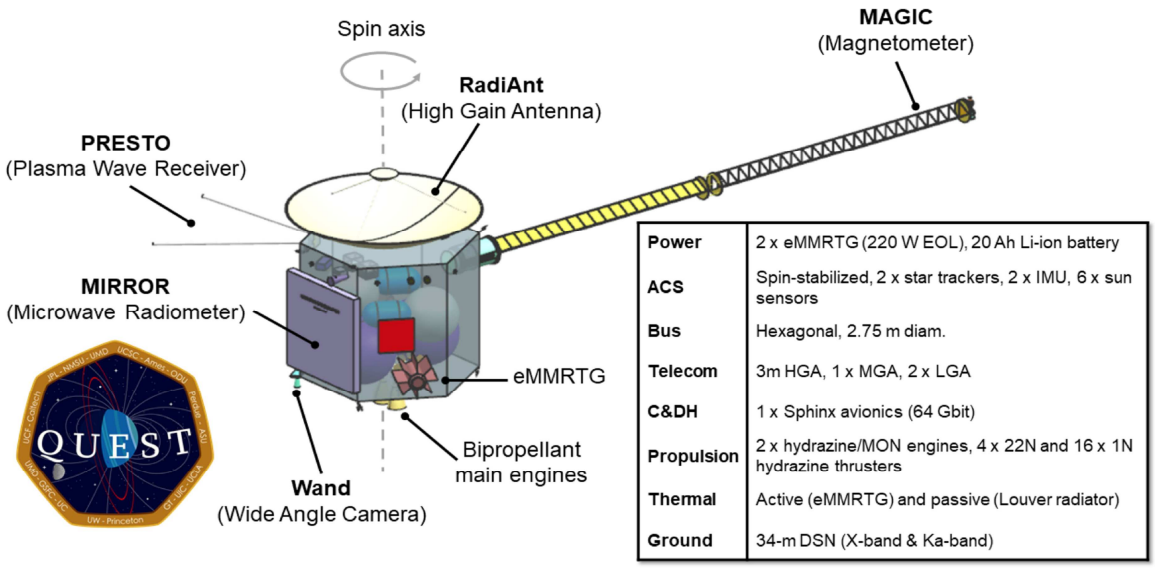

Figure 8. Baseline spacecraft schematic and summary table showing location of baseline instruments and spacecraft components.

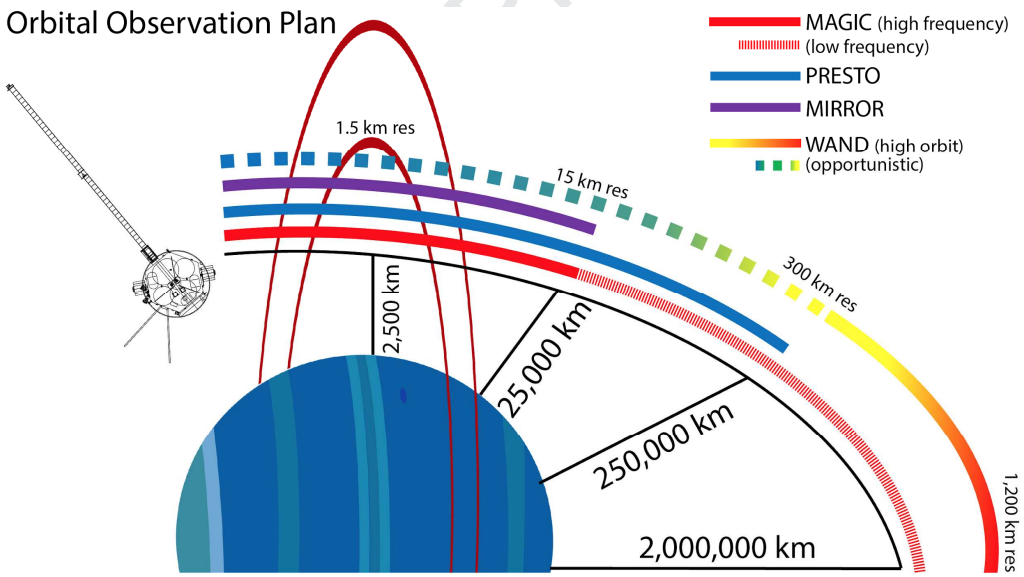

Figure 9. QUEST science operations timeline during insertion and nominal orbits.

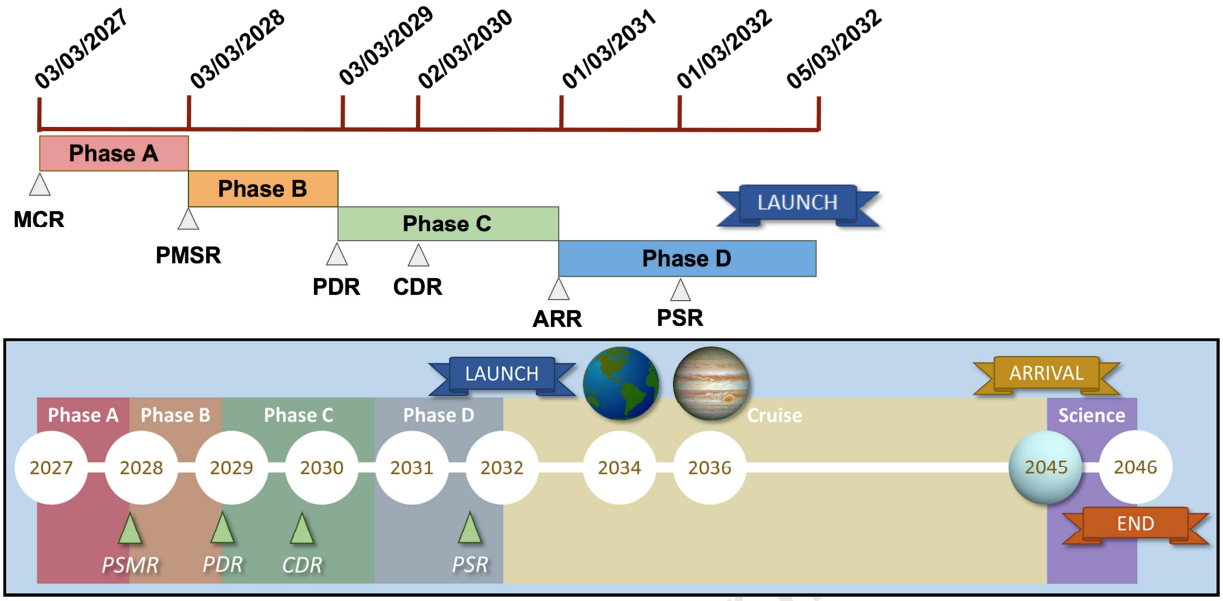

Figure 10. Notional QUEST mission schedule.

QUEST is a Uranus orbiter mission concept based extensively on the Juno mission

- The mission would address the top two objectives for a Uranus flagship mission in the NASA Decadal Survey
- The mission would investigate Uranus' unique magnetic field, atmosphere and interior environments

Declarations of interest: none